MASTER'S THESIS

Effects of Perfluorooctanesulfonic acid (PFOS) on Hypothalamic Metabolome and Testicular Function

LI, Zijie

Date of Award:
2022

HONG KONG BAPTIST UNIVERSITY

Master of Philosophy

THESIS ACCEPTANCE

DATE: March 3, 2022

STUDENT'S NAME: LI Zijie

THESIS TITLE: Effects of Perfluorooctanesulfonic acid (PFOS) on Hypothalamic Metabolome and Testicular Function

This is to certify that the above student's thesis has been examined by the following panel members and has received full approval for acceptance in partial fulfilment of the requirements for the degree of Master of Philosophy.

Chairman: Prof Wong Ricky M S
Professor, Department of Chemistry, HKBU
(Designated by Dean of Faculty of Science)

Internal Members: Prof Xiong Liming
Professor, Department of Biology, HKBU
(Designated by Head of Department of Biology)

Prof Wong Chris K C
Professor, Department of Biology, HKBU

External Examiner: Prof Lai Keng Po
Professor
Faculty of Basic Medicine
Guilin Medical University

Issued by Graduate School, HKBU

Effects of Perfluorooctanesulfonic Acid (PFOS) on Hypothalamic Metabolome and Testicular Function

LI Zijie

A thesis submitted in partial fulfillment of the requirements

for the degree of

Master of Philosophy

Principal Supervisor:

Prof. WONG Chris K C (Hong Kong Baptist University)

March 2022

DECLARATION

I hereby declare that this thesis represents my work which has been done after registration for the degree of MPhil at Hong Kong Baptist University, and has not been previously included in a thesis or dissertation submitted to this, or any other institution for a degree, diploma or other qualifications.

I have read the University's current research ethics guidelines, and accept responsibility for the conduct of the procedures following the University's Research Ethics Committee (REC). I have attempted to identify all the risks related to this research that may arise in conducting this research, obtained the relevant ethical and/or safety approval (where applicable), and acknowledged my obligations and the rights of the participants.

Signature: 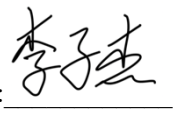

Date: March 2022

ABSTRACT

Persistent organic pollutants (POPs) are resistant to environmental degradation. In recent years, the adverse effects of these chemicals on general health have raised matters of serious public concern. Perfluorooctanesulfonic acid (PFOS) is a persistent organic pollutant and belongs to the family of poly- and per-fluoroalkyl substances (PFASs). It has been reported that PFOS can disturb the blood-testis barrier (BTB), adversely affecting the structure and function of Sertoli cells, Leydig cells and germ cells, thus disrupting the male reproductive system, reducing the testosterone level and the total sperm counts. Most of the studies examined the impact of PFOS on testicular function, while limited reports reviewed the effects of PFOS on the brain, specifically the hypothalamus, which is an integral part of the hypothalamic-pituitary-gonadal (HPG) axis. In chapter 2, we investigated the neurotoxic effects of PFOS. Immunostaining of the early response gene product c-Fos showed that PFOS activated lateral septum (LS), paraventricular nucleus of the thalamus (PVT), and the locus coeruleus (LC). No significant activation was found in the hypothalamus, such as paraventricular nucleus of the hypothalamus (PVN), medial preoptic area (mPOA), dorsomedial hypothalamus (DM), and ventromedial hypothalamus (VMH). Given the pivotal role of the hypothalamus in regulating reproductive function, we next investigated the metabolic profiling of the hypothalamus after 21 days of PFOS treatment. Principal compound analysis (PCA) showed that PFOS altered the hypothalamic metabolome. Several metabolites related to neurotransmitters and neuromodulators were altered, including N-docosahexaenoyl GABA, N-oleoyl GABA, N-palmitoyl GABA, DL-glutamate, pyroglutamic acid, D-pyroglutamic acid, L-tyrosine, and tryptophan. Kyoto Encyclopedia of Genes and Genomes (KEGG) pathway analysis showed that both 1 and 5 mg/kg PFOS altered amino acid metabolism (i.e., arginine, histidine, D-glutamine, D-glutamate, alanine, aspartate, glutamate and phenylalanine, tyrosine, and tryptophan). Metabolite set enrichment analysis (MSEA), based on the common differential metabolites, showed PFOS disturbed the metabolic pathways of the basic protein translation process, blood-brain barrier (BBB) integrity, and neurotransmitters and neuromodulators. Besides, the open field test (OFT) showed that PFOS exposed mice exhibited anxiety-like behavior as mice spent less time in the center and fewer entries to the center. In chapter 3, we evaluated the effects of 1 or 5 mg/kg PFOS on male fecundity after 21 days exposure. Results showed 5 mg/kg PFOS decreased serum luteinizing hormone (LH) levels. Furthermore, PFOS caused a decrease in caudal epididymal sperm activity. Sperm exhibited reduced curvilinear velocity (VCL), straight-line velocity (VSL), and average path velocity (VAP). Analysis of testicular transcriptome revealed that PFOS altered gene expression involved in spermatogenesis and steroidogenesis. Testicular transcriptome analysis showed that PFOS altered gene expression involved in spermatogenesis and steroidogenesis. Taken together, our results suggested that PFOS altered hypothalamic metabolome, reduced reproductive hormone levels, disrupted the process of spermatogenesis and steroidogenesis, and reduced sperm activity.

ACKNOWLEDGMENTS

I would like to express my sincere gratitude to my supervisor Prof. Chris KC WONG, for his patience, guidance and support during my study period.
I would like to express my sincere gratitude to Prof. Lei LI from Shenzhen Institute of Advanced Technology, Chinese Academy of Sciences, for her kind co-supervision, support, and encouragement during my study period.
I also want to express my sincere gratitude to Prof. Keng Po LAI for his guidance and advice.
I also want to thank Dr. Jamie HT Wan, Ziyi LIN, Shuqin JI, and Feng SHI for their valuable support and help.
I would like to thank all the scientific officers and office staff in the Department of Biology, HKBU.

Last but not least, I would like to thank my family and friends for their love and support.

TABLE OF CONTENTS

LIST OF FIGURES

LIST OF TABLES

LIST OF ABBREVIATIONS

POPs	Persistent organic pollutants
DDT	Dichlorodiphenyltrichloroethane
PFOS	Perfluorooctanesulfonic acid
HBCD	Hexabromocyclododecane
EDCs	Endocrine-disrupting chemicals
EPA	Environmental Protection Agency
PFASs	Per- and polyfluoroalkyl substances
PFOA	Perfluorooctanoic acid
EFSA	European Food Safety Authority
HAS	Human serum albumin
TWI	Tolerable weekly intakes
MAC	Maximum acceptable concentration
L-FABP	Liver fatty acid binding protein
T3	Triiodothyronine
Acox1	Acyl-coenzyme A oxidase 1
Cyp4a22	Cytochrome P450 4A22
PPARα	Proliferator-activated receptors α
ALP	Alkaline Phosphatase
AST	Aspartate aminotransferase
ALT	Alanine aminotransferase
SOD	Superoxide dismutase
GSH-Px	Glutathione peroxidase
UN	United Nations
WHO	World Health Organization
KS	Klinefelter syndrome
Tex11	Testis expressed 11
ART	Assisted reproductive technology
IVF	In vitro fertilization
BTB	Blood-testis barrier
HPG	Hypothalamic-pituitary-gonadal axis
GnRH	Gonadotropin-releasing hormone
FSH	Follicle-stimulating hormone
FSHr	Follicle-stimulating hormone receptor
LH	Luteinizing hormone
LHr	Luteinizing hormone receptor
GPR54	G-protein-coupled receptors
HH	Hypogonadotropic hypogonadism
ARC	Arcuate nucleus
POA	Preoptic area
ISH	In situ hybridization
ICC	Immunocytochemistry

DHT	Dihydrotestosterone
GnIH	Gonadotropin-inhibiting hormone
GPR147	G-protein coupled receptor 147
DM	Dorsomedial hypothalamus
LS	Lateral septal nucleus
mPOA	Medial preoptic area
PVT	Paraventricular thalamic nucleus
PVN	Paraventricular nucleus of the hypothalamus
VMH	Ventromedial hypothalamus
PCA	Principal compound analysis
KEGG	Kyoto Encyclopedia of Genes and Genomes
MSEA	Metabolite set enrichment analysis
BBB	Blood-brain barrier
OFT	Open-field test
ERK	Extracellular-signal-regulated kinase
HPA	Hypothalamic-pituitary-adrenal
CRH	Corticotropin-releasing hormone
ACTH	Adrenocorticotropic hormone
GCs	Glucocorticoids
AVP	Vasopressin
GRs	Glucocorticoid receptors
IMO	Immobilization stress
IGF-1	Insulin growth factor-1
VO	Vaginal opening
DEHA	Dehydroepiandrosterone
StAR	Steroidogenic acute regulatory protein
Cyp11a1	Cytochrome P450 Family 11 Subfamily A Member 1
Cyp17a1	Cytochrome P450 Family 17 Subfamily A Member 1
Hsd3β	3β-Hydroxysteroid dehydrogenase
Hsd17β	17β-Hydroxysteroid dehydrogenase
MAPK	Mitogen-activated protein kinases
JAM	Junctional adhesion molecule
GJ	Gap junction
H3K18ac	Histone 3 at lysine placed on position 18
H3K9ac	Acetylation of histone 3 at lysine placed on position 9
ROS	Reactive oxygen species
TNF-α	Tumor necrosis factor-α
CaMKII	Calcium/calmodulin-dependent protein kinase II
GAP-43	Growth-associated protein-43
SYP	Synaptophysin
ERα	Estrogen receptor α
AFFF	Aqueous film-forming foam
VCL	Curvilinear velocity
VSL	Straight-line velocity

VAP	Average path velocity
MTBE	methyl tert-butyl ether
TBA	Tetrabutylammonium hydroxide solution
CASA	Computer-assisted sperm analysis
ANOVA	One-way analysis of variance
Arp3	Actin-related protein 3
Mylk	myosin light chain kinase
ML-9	1--1H-hexahydro-1,4-diazepine hydrochloride
RCR	Respiratory control ratio
β-CD	Methyl-β-cyclodextrin
TG	Triglyceride
PUFAs	Polyunsaturated fatty acids
DHA	Docosahexaenoic Acid
SON	Supraoptic nucleus
SCN	Suprachiasmatic nucleus
ADHD	Attention-Deficit/Hyperactivity Disorder
PFA	Paraformaldehyde
PBS	Phosphate-buffered saline
DAPI	4',6-diamidino-2-phenylindole, 0.4 μg/mL, Sigma
UPLC	Ultra-performance liquid chromatography
M/Z	Mass-to-charge ratio
HMDB	Human Metabolome Database
AaRSs	Aminoacyl-tRNA synthetases
ABC	ATP-binding cassette
qPCR	Quantitative real-time PCR
CCV	Renal clearance values
Kiss1R	Kisspeptin receptors
GnIH-ir	GnIH-immunoreactive
GO	Gene Ontology
Dync1h1	Cytoplasmic dynein 1 heavy chain 1
Rimbp3	RIMS binding protein 3
Cfap44	Cilia and flagella associated protein 44
Dnaic2	Dynein, axonemal, intermediate chain 2
Dnah10	Dynein, axonemal, heavy chain 10
Nup210l	Nucleoporin 210 like
FPKM	Fragments Per Kilobase of exon model per Million mapped fragments
GAPDH	Glyceraldehyde-3-phosphate dehydrogenase

Chapter 1 literature review

1.1. Persistent organic pollutants (POPs)

Persistent organic pollutants (POPs) are organic substances resistant to photolytic, biological, and chemical degradation. They are characterized by hydrophobicity, lipophilicity, semi-volatility, and bioaccumulation [1]. POPs were commonly found in commodity and industrial products, including chlordane, dichlorodiphenyltrichloroethane (DDT), perfluorooctanesulfonic acid (PFOS), and hexabromocyclododecane (HBCD). Pesticides chlordane and DDT were once popular. PFOS was found in firefighting foam, fibre protector, and food packaging coatings, and HBCD was used for building insulation. All of which have been listed on the Stockholm Convention list of Persistent Organic Pollutants by the United Nations Environment Programme. According to the U.S. Environmental Protection Agency (EPA), some POPs are also members of endocrine-disrupting chemicals (EDCs) that can interfere with the endocrine system by disrupting the synthesis, secretion, transport, binding, or elimination of hormones [2]. EDCs can bind to hormone receptors, including estrogen receptors, androgen receptors, and glucocorticoid receptors, adversely impacting hormonal signaling [2]. Moreover, emerging studies show that EDCs can bind to neurotransmitter receptors and orphan receptors [3]. EDCs exposure has been linked to various health risks, including increased carcinogenic incidence, reproductive dysfunction, neurotoxicity, and immunotoxicity [1,4].

1.1.1. Per- and polyfluoroalkyl substances (PFASs)

The per- and poly-fluoroalkyl substances (PFASs) are organofluorine compounds with carbon-carbon bonds and carbon-fluorine bonds. Hydrogen atoms are replaced by fluorine atoms. The caron-fluorine bond is highly stable; as a result, PFASs are persistent and resistant to degradation (Fig 1.1) [5]. Due to their unique chemical and thermal stability, PFASs were widely used in the commercial and industrial sectors. For example, PFASs were common in food packages, stain- and water-repellent fabrics, fire-fighting foams, polishes, and electronics manufacturing [6]. According to the toxicity database DSSTox of the U.S. Environmental Protection Agency (EPA), there are more

than 8,000 different PFASs. The two most studied chemicals of the PFASs family are perfluorooctanoic acid (PFOA) and perfluorooctaneousulfonic acid (PFOS), both of which belong to the C8 PFASs family.

1.1.2. Perfluorooctanesulfonic acid (PFOS)

The carbon-fluorine bonds structure of perfluorooctanesulfonic acid (PFOS) makes it hydrophobic and lipophobic, and the sulfonic acid group is hydrophilic (Fig 1.2). In 1949, PFOS was first used in the textile industry as a fabric protector 'Scotchgard' by 3M company. Later, PFOS was also commonly used in textile impregnation agents, polishing agents, metal plating, and firefighting foams. In 1968, fluorinated organic compounds were detected in human blood [7]. In 1999, the U.S. Environmental Protection Agency surveyed the global distribution and potential toxicity of PFOS. Subsequently, 3M ceased manufacturing PFOS and its related products in 2000. The Stockholm Convention on persistent organic pollutants listed PFOS and its salts in Annex B in 2009. Although it has been phased out in industrial and commercial areas, the stable structure and large-scale application led to wide distribution in the environment. PFOS can be directly released into the soil, air, and water during manufacturing,. Moreover, there are remaining impurities and residuals in PFOS-based products, which can be the precursor to PFOS. Biological and abiotic environmental processes can transform precursors into PFOS [8].

There were reports about the distribution of PFOS in the environment. The concentration of PFOS in Antarctic coastal waters ranged from 2 ng/L to 600 ng/L [9]. PFOS level in landfill leachate in Guangzhou was approximately 500 ng/L [10]. It was estimated that 70% to 80% of PFOS in China came from industrial sewage [10]. Liu et al. examined the PFOS level in drinking water. Results showed that Lianyungang, Shenzhen, and Dongguan residents were exposed to 186.17 ng/L, 9.954 ng/L, and 24.227 ng/L PFOS, respectively [11].

1.1.2.1. Existence and distribution of PFOS in human and animals

In the food chain, higher-trophic-level organisms have higher concentrations of PFOS because PFOS is bio-accumulative [12]. It is known that people are exposed to PFOS through ingestion, respiration, and occupation [13]. An epidemiology study in Xinjiang reported that PFOS was detected

in 93% of blood specimens with median levels of 2.39 μg/L in males and 1.93 μg/L in females [14]. PFOS also was detected in breast milk; for example, the geometric mean concentrations of PFOS in breast milk were 46 pg/mL in mainland China [15]. In Spain, the levels of PFOS in cord plasma were 1.17 ng/mL. These data indicated newborn exposure to PFOS through the placenta and breast milk [13]. According to the European Food Safety Authority (EFSA), the PFOS concentrations were 7.7 ng/mL in adults and 3.2 ng/mL in children [16].

An epidemiology study showed that human serum albumin (HAS), one of the major proteins in human plasma, can bind with PFOS at a molar ratio of 2:1 and alter the conformation of HAS [17]. Because of the high affinity of PFOS, its half-life ranges from 4.5 to 7.4 years in humans [18]. On the contrary, elimination of PFOS was less efficient than absorption. There are two main ways to remove absorbed PFOS, one through excretion and the other through bile. In 2014, Zhou et al. assessed occupational exposure to PFAS in Tangxun Lake, Wuhan, and determined the renal clearance values (CCV), a substance's rate of clearance from the body, for PFOS vary from 0.002 to 0.091 mL/day/kg [19]. Another study determined the CCV for PFOS was average at 0.012 mL/day/kg for men and 0.019 mL/day/kg for women [20]. Besides, the epidemiology study found that people aged 12-19 with high levels of PFOS exhibited reduced glomerular filtration rate (GFR) and increased serum uric acid [21]. As for biliary excretion, the PFOS excretion rate in bile ranged between 1.06 and 2.98 mL/kg/day higher than in urine [22]. However, the biliary reabsorption rate for PFOS was 0.97, which means that the majority of excreted PFOS from bile could be reabsorbed by the digestive tract [22]. The hazardous effect of PFOS has caught the attention of global health departments. European Food Safety Authority (EFSA) sets up tolerable weekly intakes (TWI) of 13 ng/kg body weight per week [23]. Health Canada established a maximum acceptable concentration (MAC) for PFOS in drinking water of 0.6 μg/L. The U.S. Environmental Protection Agency (EPA) sets drinking water health adversaries of 0.07 ng/L for PFOS.

The body absorbed PFOS with a high affinity to albumin, globulin, and liver fatty acid-binding protein (L-FABP). Animal studies showed a high level of PFOS in rat liver because PFOS binds to L-FABP [24]. As a result, the liver is one of the primary targets. The hepatic effects of PFOS have been well studied. In 2002, Seacat et al. evaluated the toxic effects of PFOS on primates using cynomolgus monkeys (*Macaca fascicularis*) fed with 0.03, 0.15, and 0.75 mg/kg PFOS for 182 days

[25]. Results showed that 0.75 mg/kg PFOS treated animals exhibited increased liver weight, reduced body weight, decreased serum cholesterol, and triiodothyronine (T3). Histologically, hepatocellular hypertrophy and lipid vacuolation was found in the 0.75 mg/kg group [25]. The increased liver weight was also observed in the rodent models. Sprague–Dawley rats treated with PFOS exhibited hepatomegaly and up-regulated gene expression of acyl-coenzyme A oxidase 1 (*Acox1*) and cytochrome P450 4A22 (*Cyp4a22*) in the liver [26]. It has been found that PFOS could alter lipid metabolism by activating peroxisome proliferator-activated receptors α (PPARα), a kind of nuclear receptor. The incitation of PPARα could increase the number of peroxisomes and inhibit the peroxisomal beta-oxidation in hepatocytes [27,28]. The inhibition of peroxisomal beta-oxidation will disrupt the citric acid cycle and cause the aggregation of fatty acids and triglycerides in hepatocytes. Besides, oxidative stress also accounts for hepatotoxicity. A study in male C57BL/6J mice found that 0.15 or 0.3 mg/kg PFOS exposure for 30 days increased serum alkaline phosphatase (ALP), aspartate aminotransferase (AST), and alanine aminotransferase (ALT) levels and decreased hepatic superoxide dismutase (SOD), catalase, and glutathione peroxidase (GSH-Px) levels [29]. An *in vitro* study by Khansari et al. showed that 25 μM PFOS treated rats liver cells suffered from reduced glutathione, lysosomal membrane leakiness, and cellular proteolysis [30]. Epidemiologically, Gallo et al. found a positive association between serum PFOS levels and ATL levels [31].

1.1.2.1.1. PFOS and global fertility rate decrease

According to the United Nations (UN), the global fertility rate reduced from 3.2 live births per female in 1900 to 2.5 in 2019. Globally, the level of fertility rate is expected to decrease to 2.1 in 2050 and 1.9 in 2100. In Central and Southern Asia the fertility rate declines to 1.9 births per female. In Europe and Northern America, the fertility rate falls to 0.1 births. In the highest fertility region sub-Saharan Africa, the fertility rate drops from 6.3 to 4.6 births per woman. The declining fertility rate will profoundly impact economic, social, and political development, including a reduction in the size of potential workforces and an increase in aging populations.

According to World Health Organization (WHO), infertility refers to the inability to conceive after more than 12 months of regular, unprotected sexual intercourse [32]. It is estimated that about 8-12% of couples are affected by infertility, and approximately 50% of cases are related to male infertility

[33]. Approximately 7% of males suffer from infertility [34]. An epidemiological study indicates that sperm concentration has decreased in many countries, including France, the United Kingdom, America, and Spain [35]. A systematic review reported that sperm concentrations declined 52.4% between 1973 and 2011 [36]. These results show the decline of sperm count and imply the disorder of spermatogenesis. Currently, clinical diagnosis of male infertility relies on semen and hormone analysis. WHO develops the criteria for sperm analysis from the different parameters such as quantity, morphology, and motility. The symptoms of sperm disorders are diverse, including oligozoospermia (reduced sperm count), asthenozoospermia (decreased sperm motility) and, teratozoospermia (reduced percentage of sperm with normal morphology).

Infertility is likely to hurt not only individuals but also society. Emerging studies suggest the association between oncologic diseases and male infertility. For example, a survey of 22, 562 respondents with male factor infertility from 1967 to 1998 showed that those suffering from infertility were three times more likely to develop testicular cancer than the general population [37]. It is supposed that male sex hormone protects against autoimmunity, as testosterone inhibits pro-inflammatory cytokine production, CD4-positive cells differentiation, immunoglobulin production, and natural killer cell cytotoxic activity [38]. Pressures from society and the economy may be detrimental. For example, in South Africa, people with reproductive disorders could be ridiculed as 'failure', 'castrated cow', or 'bad swimmers' [39]. Infertiles who turn to assisted reproductive technology (ART) may have to bear the financial burden as well as the social stigma. According to a study, a standard In vitro fertilization (IVF) costs on average $12,000 and $8,000 in the US and Canada, respectively [40]. Taken together, infertility influences not only individual well-being but also economic and social development.

1.1.2.1.2. PFOS disrupts the regulation of male reproductive system

Testes are responsible for sperm production and storage, androgen synthesis, and secretion. Anatomically, there are numerous seminiferous tubules inside the testes where spermatogenesis occurs. Spermatogenesis is the process by which male germ cells, spermatogonia, develop into spermatocytes [41]. There are two other types of somatic cells in the testis, one are Sertoli cells, and the other are Leydig cells. Sertoli cells are supporting cells and are responsible for nourishing and

supporting the development of sperm cells [42]. Sertoli cells are the key component of the blood-testis barrier (BTB) [43]. Leydig cells are located in the connective tissues outside the seminiferous tubules and are responsible for testosterone synthesis [44]. Immature sperm from the lumens of seminiferous tubules move into the epididymis, which is a long, coiled tube connecting the testis and vas deferens. Epididymis plays an important role in the acquisition of motility and fertilizing ability. The epididymis can be divided into three parts, caput, corpus, and cauda; each region has distinctive functions. Both the caput and the corpus parts are responsible for sperm maturation, and the cauda part serves as the reservoir of functionally mature spermatozoa [45].

The reproductive system is controlled by the hypothalamic-pituitary-gonadal (HPG) axis. At the hypothalamus level, the neurons secrete a gonadotropin-releasing hormone (GnRH) to the pituitary gland via the hypothalamic-hypophysial-portal vessels and control the release of follicle-stimulating hormone (FSH) and luteinizing hormone (LH) in the anterior pituitary. GnRH is the decapeptide that was clarified by Roger Guillemin and Andrew V. Schally in 1971. Most vertebrates have at least two forms of GnRH, GnRH-I and GnRH-II. They are encoded by two different genes [46]. In 1978, belchetz et al. found that both FSH and LH release with a pulsatile pattern in the female rhesus monkeys [47]. Gonadotropins (FSH and LH) concentrations in the circulation were normal depending on GnRH administration once an hour in rhesus monkeys with the hypothalamic lesion. However, persistent GnRH administration failed to stimulate gonadotropin release [47]. 'GnRH pulse generator' was used to describe pulsatile GnRH release from GnRH neurons. As for the positive regulation of upstream of 'GnRH pulse generator'. In 2003, the role of kisspeptin, a 54 amino acid peptide encoded by the *Kiss1* gene in humans, as a neuropeptide was reported independently by two groups from the US and France [48,49]. There are kisspeptin receptors (Kiss1R)/G-protein-coupled receptors (GPR54) expressed on the GnRH neurons. *Gpr54* knockout mice exhibited hypogonadotropic hypogonadism (HH) and infertility [50]. As for males, HH refers to reduced testicular functions with disturbed spermatogenesis and steroidogenesis [51]. Patients with inactivating *Kiss1* mutation suffered from hypogonadotropic hypogonadism [52]. The distribution of kisspeptin cells is not the same among species. In humans and rats, the arcuate nucleus (ARC) and preoptic area (POA) house kisspeptin cells. In mice, in situ hybridization (ISH) and immunocytochemistry (ICC) showed kisspeptin neurons located in the ARC, anteroventral periventricular nucleus (AVPV), and median eminence

(ME) [53]. Dynorphin A belongs to endogenous opioid peptides, which share the common amino acid sequence Tyr-Gly-Gly-Phe-Leu [54]. The receptor of dynorphin A is known as Gi-coupled inhibitory GPCRs [54]. Goodman and his colleagues found that dynorphin A plays an important role in the progesterone-negative feedback in ewes [55]. Recently, co-localization of neurokinin B and dynorphin A in ARC kisspeptin neurons has been proved in mice [56], rats [57], and goats [57]. Neurons with co-expression of kisspeptin, neurokinin B, and Dynorphin A are called KNDy neurons. It is proposed that KNDy neurons regulate GnRH pulsatile secretion, in which neurokinin B acts as stimulation, dynorphin A acts as inhibition [58]. Among the negative regulators upstream of the GnRH pulse generator, Gonadotropin-inhibiting hormone (GnIH) is the peptide that can inhibit gonadotropins secretion. Glucocorticoids (GCs) play a stimulatory role in GnIH expression. There are glucocorticoid receptors (GRs) presented on GnIH neurons in quails, and GCs treatment can upregulate GnIH mRNA levels [59]. GnIH inhibits FSH and LH synthesis by inhibiting GnRH neurons and gonadotropes via G-protein coupled receptor 147 (GPR147) [60]. GnIH was first isolated and identified in birds in 2000 by Tsutsui's group [61]. GnIH regulates the reproductive system at different levels. Immunocytochemistry shows that GnIH-immunoreactive (GnIH-ir) cells were housed in the dorsomedial hypothalamus (DM) in rodents [62]. Immunocytochemistry also showed that GnIH-ir neuronal fibres were distributed in the lateral septal nucleus (LS), medial preoptic area (mPOA), paraventricular thalamic nucleus (PVT), and Paraventricular nucleus of hypothalamus (PVN)[62]. Ubuka et al. found that GnRH neurons express GPR147 and receive inputs from GnIH neurons [63]. An *in vitro* study found that GnIH can inhibit the GnRH-induced LH secretion by acting on the extracellular-signal-regulated kinase (ERK) signaling pathway [59].

At the pituitary level, GnRH binds to the cognate receptor expressed in gonadotrophs which secrete FSH and LH in response. Both FSH and LH are released into the blood and transported to the gonad (ovary and testis). At the gonadal level, the ovary and testis can synthesize and secrete estrogen, progesterone, and androgen. In males, LH binds to Leydig cells and stimulates testosterone production, FSH acts on Sertoli cells. In turn, these steroids secreted by the gonads can inhibit hypothalamic GnRH, pituitary LH, and FSH synthesis.

The hypothalamic-pituitary-adrenal (HPA) axis is another neuroendocrine system that processes stress and maintains homeostasis. There is a reciprocal relationship between the HPA axis and the

HPG axis. The hormones involved in the HPA axis include corticotropin-releasing hormone (CRH), adrenocorticotropic hormone (ACTH), and glucocorticoids (GCs) [64]. The paraventricular nucleus of the hypothalamus (PVN) produces corticotropin-releasing hormone (CRH) and vasopressin (AVP). CRH is transported to the anterior pituitary and stimulates the secretion of adrenocorticotropin (ACTH), which then stimulates the release of glucocorticoids (cortisol in humans, corticosterone in mice and rats) from the adrenal gland. GCs are involved in the flight-fight responses, increase the possibility of survival, and save energy by reducing some metabolic processes, which include reproduction [65]. The glucocorticoids (GCs) bind to glucocorticoids receptors (GRs) expressed in CRH neurons, pituitary, and testes and affect the function of the HPG axis [66]. Immunohistochemistry showed the colocalization of CRH receptors and GRs on kisspeptin neurons, and GCs administration decreased *kiss1* mRNA levels in male mice [67]. At the pituitary level, GCs can inhibit LH secretion and promote FSH secretion [68,69]. At the gonadal level, Leydig cells, macrophages, and fibroblasts expressed GRs [70]. GCs can inhibit the transcription of genes involved in steroidogenesis, such as cytochrome P450-dependent cholesterol side-chain cleavage enzyme (P450scc) and cytochrome P450-dependent 17alpha-hydroxylase/C17-C20 lyase (CYP17A1) [70]. Rats treated with immobilization stress (IMO) for two hours exhibited increased serum corticosterone and adrenaline levels and an increased number of apoptotic Leydig cells [71].

1.1.2.1.2.1. PFOS disrupts steroidogenesis and spermatogenesis

PFOS is a kind of endocrine-disrupting chemical (EDC) that plays an adverse role in reproduction. Epidemiology studies found the possible connection between neonatal or juvenile exposure to PFOS and the development of the reproductive system. A cross-sectional analysis in 6-9 year old boys found that serum PFOS concentrations are inversely associated with Insulin growth factor-1 (IGF-1), testosterone, and estradiol levels [72]. A study of 8-18 year old boys found an inverse association between serum PFOS levels and the age of puberty [73]. Du et al. found that neonatal PFOS exposure at 1 or 10 mg/kg results in advanced puberty onset, including an advanced vaginal opening (VO) and first estrus, and *Kiss1* and *Gpr54* mRNA expression in the hypothalamus were suppressed in female rats [74]. Another study examined the effect of in utero exposure to 5 and 20 mg/kg PFOS from GD1 to GD19 and observed that the rats exhibited decreased testosterone levels and a decreased number of fetal Leydig cells [75]. These results suggested that PFOS could impair the male

reproductive system at developmental stages.

Leydig cells and Sertoli cells are two key somatic cells in the testes, both of which are the targets of PFOS. Leydig cells are responsible for testosterone, androstenedione, and dehydroepiandrosterone (DHEA) synthesis. The steroidogenic acute regulatory protein (StAR), cytochrome p450 family 11 subfamily A member 1 (CYP11A1), 3β-hydroxysteroid dehydrogenase (3β-HSD), and 17β-hydroxysteroid dehydrogenase (17β-HSD) participate in steroidogenesis. Quantitative real-time PCR (qPCR) results showed after 21-day PFOS treatment, steroidogenic enzyme genes expressions such as *Star*, *Cyp11a1, Cyp17a1, Hsd3β*, and *Hsd17β* were decreased [76]. In line with reduced gene expression of several steroidogenic key enzymes, reduced serum testosterone concentrations and epididymal sperm counts occurred after 21-day 10 mg/kg PFOS treatment [76]. Another extended 5-week treatment with 10 mg/kg PFOS also reduced testes weights and sperm counts in mice. [77].

Sertoli cells support and nourish the developing immature germ cells in the seminiferous tubules. The tight-junctions formed by Sertoli cells divide the seminiferous epithelium into the basal and adluminal compartments, providing the immune privilege for the germ cells [78]. The adverse effects of PFOS on Sertoli cells have been reported. An *in vitro* study showed that activation of the p38 mitogen-activated protein kinases (MAPK) pathway in primary CD-1 mice Sertoli cells followed PFOS treatment, the Sertoli cells tight-junction was perturbed, and proteins involved in BTB such as junctional adhesion molecule (JAM), occludin, claudin 11, connexin 43 were reduced [79,80]. Another *in vitro* study showed that 5-10 g/mL PFOS disrupted rats' Sertoli cells F-actin organization and decreased expression of connexin-43 involved in inter-Sertoli cell gap junction (GJ) communication resulting in BTB disruption [81]. Transcriptome and immunocytochemical staining revealed the global cytotoxicity caused by PFOS to Sertoli cells in the aspects of cytoskeleton signaling, cell-cell junction, and inflammation [82].

It has been reported that PFOS altered the rats' testicular transcriptome and interrupted signaling of Sertoli cells tight junctions and spermatocytes-Sertoli cells junctions. In a chronic 0.015 or 0.15 mg/kg PFOS exposure for 60 days, results showed steroidogenic gene expression was altered, for example, *Star*, *Cyp11a1*, and *Hsd3β* were up-regulated, but *Cyp17a1* and *Hsd17β* were down-regulated, which led to increased testosterone levels [83]. Acetylations of histone 3 at lysine on position 18 (H3K18ac) as well as acetylation of histone 3 at lysine on position 9 (H3K9ac) were

observed in the promoter of *Cyp11a1* and *Hsd3*, respectively. The accumulation of H3K18ac and H3K9ac led to the activation of steroidogenic gene expression (*Cyp11a1* and *Hsd3β*) [50]. In another study of chronic 0.1 mg/kg PFOS for 4 months, decreased StAR protein expression and reduced H3K14ac were observed [84].

Taken together, PFOS can disrupt BTB integrity and impair spermatogenesis and steroidogenesis resulting in infertility.

1.1.2.1.2.2. PFOS disrupts Hypothalamic–pituitary–gonadal (HPG) axis

Studies have shown that exposure to PFOS causes adverse effects on the nervous system. PFOS existence in the wildlife brain has been reported [85-87]. Studies determined the distribution of PFOS in rats or mice and showed PFOS existence in the brain [88-90]. An *in vitro* experiment found that PFOS induced disassembly of endothelial tight junctions through the phosphatidylinositol-3 kinase/Akt-pathway [91]. The blood-brain barrier (BBB) consists of endothelial cells, astrocytes, and pericytes, which acts as the physical barrier and selective transport interface [92]. Another study showed that PFOS disrupted BBB by reducing the expression levels of proteins ZO-1, Claudin-5, and Occludin in the endothelial cells [88]. Chen et al. studied the neurotoxic effect of PFOS using SH-SY5Y cells and showed 12.5 mg/L PFOS caused cell apoptosis with increased reactive oxygen species (ROS), lipid peroxidation, superoxide dismutase activity, and a decreased glutathione peroxidase activity [93]. These results suggested that PFOS can impair BBB by reducing TJ-related protein levels and inducing cell apoptosis. Besides, it has been reported that PFOS can induce neuroinflammation. An *in vitro* study found that PFOS can induce excessive secretion of pro-inflammatory cytokines tumor necrosis factor-α (TNF-α) in astrocytes [94]. Excessive secretion of the inflammatory cytokines can impair the nervous system [95]. Disrupted Synapse formation and synaptic plasticity have been found after PFOS treatment. Mice treated with PFOS at a single dose of 11.3 mg/kg on postnatal day 10 exhibited increased CaMKII, GAP-43, and synaptophysin expression in the hippocampus [96]. Hippocampus is involved in memory and learning. This serine/threonine-specific protein kinase CaMKII is expressed in the postsynaptic density and plays an important role in the molecular mechanism of memory formation. [97]. GAP-43 is involved in the regulation of axon terminal growth, overexpression of GAP-43 results in the spontaneous formation of new synapses. On the other hand, depletion of GAP-43 leads to neurite and growth cones

formation [98]. SYP is an integral membrane glycoprotein and expressed in presynaptic vesicles, but the function of SYP remained unclear [99]. It is proposed that SYP is involved in the regulation of the kinetics of synaptic vesicle endocytosis in neurons [100]. An *in vitro* study found that SYP can be phosphorylated by CaMKII [101]. Liu et al. showed that adult male rats administered with 1.7 mg/L PFOS in drinking water for three months exhibited increased CaMKII expression in the cortex and the hippocampus [102]. Animal studies have found that PFOS treatment can cause impairment in learning and spatial memory. Animals fed with 10.75 mg/kg PFOS for three months experienced cell apoptosis in the hippocampus, and their spatial learning and memory were impaired [103]. PFOS alters calcium homeostasis in neurons by disrupting the calcium ion channel, which results in extracellular calcium influx and intracellular calcium release, and the release of neurotransmitters into synaptic clefts [104]. Male adult rats treated with PFOS for 28 days exhibited increased norepinephrine (NE) levels in the PVN of the hypothalamus [89]. Foguth et al. found that the PFOS exposure could decrease brain dopamine levels in the northern leopard frogs [105]. These results suggested that PFOS can impair the nervous system by altering neuron activity and the release of neurotransmitters. The hypothalamus is the core of the neuroendocrine system. Wang et al. found that PFOS caused diestrus prolongation and ovulation reduction in adult mice by repressing kisspeptin neurons in the hypothalamus AVPV nucleus. [106]. Du et al. found that neonatal or juvenile PFOS exposure suppressed gene expression of estrogen receptor α (*Erα*), *Kiss1*, and *Gpr54* [74]. These results indicated that PFOS might alter the hypothalamic control of reproduction. Taken together, PFOS perturbs BBB and acts adversely on glial cells and neurons, including neuroinflammation, disturbing intracellular calcium homeostasis and neurotransmitter release.

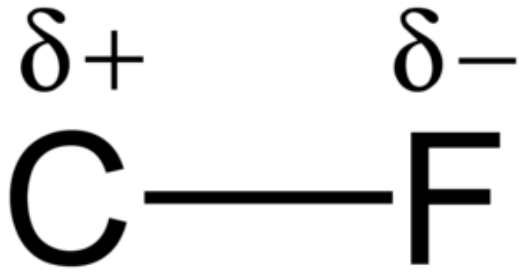

Fig 1.1 Carbon-fluorine bonding

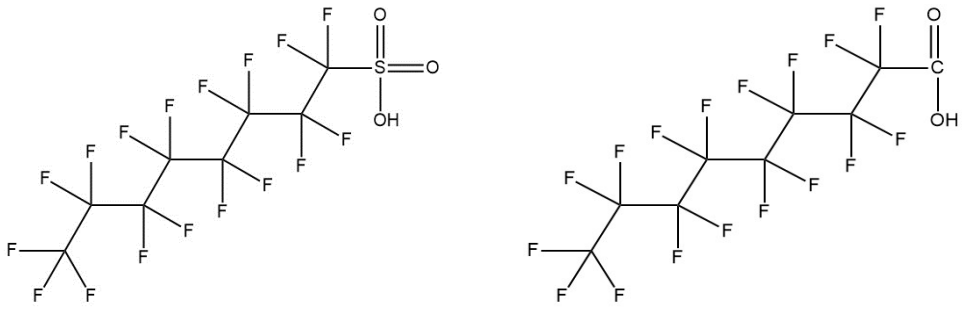

Perfluorooctanesulfonic acid (PFOS) Perfluorooctanoic acid (PFOA)

Fig 1.2 Structural Formula of PFOS and PFOA

Aims of the study

It is known that PFOS can induce reproductive toxicity. Piles of studies elucidated that PFOS can disrupt the reproductive system at the gonadal level. Recently, emerging evidence has suggested that PFOS can disrupt the blood-brain barrier (BBB) and cause neurotoxicity. In general, reproduction is controlled by the nervous system, particularly the hypothalamus-pituitary-gonadal (HPG) axis. As a result, PFOS may adversely affect cerebral signals, impairing the HPG axis more systematically. Here we set up two aims in the study:

1. To characterize the effects of PFOS on brain nuclei targets and the hypothalamic metabolome.
2. To investigate the effects of PFOS on male fecundity with reference to sperm quality.

Chapter 2 PFOS altered the hypothalamic metabolome and caused anxiety-liked behavior

2.1 Introduction

It is believed that PFOS is neurotoxic, causing damage to the nervous system and affecting its structure and function. It has been reported PFOS affected the locomotion, spatial learning, and memory of the animals [103,107,108]. As reproductive functions are closely controlled by the CNS, notably the hypothalamus-pituitary-gonadal (HPG) axis. Thus, it is possible that the adverse effects of PFOS on male fecundity are not restricted to local testicular signaling alone, or are more systematic, including effects on cerebral signaling. The hypothalamus is located bellowed the thalamus and on the undersurface of the brain, playing a key role in the endocrine system. Anatomically, it can be divided into three major regions: anterior, middle and posterior region, each consisting of different hypothalamic nuclei serving different physiologic functions [109]. The anterior region contains the preoptic area (POA), paraventricular nucleus (PVN), supraoptic nucleus (SON), suprachiasmatic nucleus (SCN), and anterior hypothalamic nucleus. The middle region contains arcuate, ventromedial nucleus (VMH), and dorsomedial nucleus (DM). The posterior region is composed of mammillary nuclei and posterior hypothalamic nucleus.

It has been reported that PFOS affects the hypothalamus, the core of the HPG axis. López-Doval et al. investigated the PFOS effects on adult male rats and showed 28 days of PFOS exposure down-regulated gene expressions of *Gnrh, Lh and Fsh* in the brain [110]. Wan et al. determined the gene expressions (*Kiss1, Gpr54,* and *Gnrh*) levels in the male CD-1 mice hypothalamus after 21-day PFOS (1 and 5 mg/kg) exposure, and results showed no significant difference [76]. The expressions of the *gnrh*, *fsh*, and *gnrhr* genes in zebrafish significantly decreased following exposure to 220 μg/L or 200 μg/L PFOS [111]. Another study on male rats found that PFOS reduced hypothalamic luteinizing hormone receptor (LHr) protein levels in 3 and 6 mg/kg groups and follicle-stimulating hormone receptor (FSHr) protein levels in 1, 3, and 6 mg/kg groups [112]. As hypothalamic circuitry is complex, several studies assessed the PFOS

effect on hypothalamic nuclei. A significant increase in NE levels was observed in the paraventricular nucleus of the hypothalamus (PVN) of female rats treated with 10 mg/kg PFOS for two weeks [89]. Furthermore, S. López-Doval et al. found NE increase in the anterior hypothalamus and posterior hypothalamus of male SD rats after PFOS exposure [110]. In addition, it has been reported that neonatal or juvenile exposure to PFOS disturbs the kisspeptin system in the POA and ARC of female mice [74]. Similar results were found in adult female mice as PFOS suppressed kisspeptin neurons in the AVPV and caused prolonged diestrus [106]. Many studies on the hypothalamic effect of PFOS use female mice or rats as animal models. Few studies have examined the effects of PFOS on the brain of male animals.

A recent study reported that PFOA affected serotonin, dopamine, norepinephrine, and glutamate levels in the male Balb/c mice brain by metabolomic analysis [113]. The toxic effects of PFOS on the nervous system resulted in deranged spontaneous behavior, as shown in different animal models. Johansson et al. determined locomotion, rearing, and the total activity of 4-month-old mice fed with 21 μmol/kg PFOS at the age of 10 days [114]. Results showed all these parameters were significantly reduced in adult mice. Similar effects have also been detected by Onishchenko et al. in C57BL/6/Bkl mice [115]. Epidemiologically, Hoffman et al. investigated the underlying association between polyfluoroalkyl chemicals (PFCs) and attention-deficit/hyperactivity disorder (ADHD) in American children and suggested children with higher serum PFCs levels have increased odds of ADHD [116]. Domingo et al. assessed the effects of a month of PFOS exposure on mice's behavior [117]. Results showed 3 mg/kg PFOS exposure caused anxiety-like behavior in the open field test (OFT) as animals spent less time in the central zone with a downward trend in the ratio of the distance moved in the center. In a recent study, exposure to 200 μg/L PFOS impaired standard zebrafish sexual behaviors, including chasing, nose-tail, and tail-touching [111]. Piles of studies investigated the PFOS effects on neurobehavior during prenatal or before adulthood, but less reported on adult exposure. In this study, we reported finding that PFOS accumulation in the hypothalamus and the disrupted metabolic pathway were distinguished through metabolomic analysis. Possible brain nuclei activation was studied using c-Fos immunostaining. Besides, we also found PFOS causes anxiety-like behavior in mice.

2.2 Material and Methods

2.2.1 Animals

6 week-old male CD-1 mice (Zhejiang Vital River Laboratory Animal Technology Co., Ltd) were grouped-housed with 12:12-h light/dark cycle. The animals were fed with food pellets and water *ad libitum*. All husbandry and experimental procedures in this study were approved by the Animal Care and Use Committee of the Shenzhen Institute of Advanced Technology, Chinese Academy of Sciences, China. The mice were randomly divided into three groups (10~15 individuals per group). Perfluorooctanesulfonate acid (PFOS, 98% purity, Shanghai ZZBIO Co., Ltd, China) was dissolved in dimethyl sulfoxide (D5879-1L, Sigma, USA) prior to mixing with corn oil (C7030, Solabio, China). The mice were weighed and orally administered 1 or 5 mg/kg PFOS in corn oil by gavage daily in the morning for 21 days. Body weight was recorded every other day. On day 21, the mice were subjected to an open field test (OFT). The mice were then anesthetized with an intraperitoneal injection of pentobarbital at a dosage of 50 mg/kg. Hypothalamus was harvested for LC-MS/MS analysis and metabolomic analysis.

2.2.2 LC-MS/MS analysis of PFOS concentrations

After the 21-day treatment, blood, epididymis, and brain tissues were subjected to PFOS content analysis by LC-MS/MS. Briefly, tissues were mixed with internal standard (PFOS, purity > 98%, MPFACMXA0714, Wellington Laboratories, Canada), 0.5 M TBA, and 0.25 M sodium carbonate buffer. Then, the mixture was placed in an orbital shaker at 250 rpm for 20 min. After centrifugation at 3000 rpm for 15 minutes, the organic layer was transferred to a new tube. All of the organic fractions were pooled after repeated extractions. Drying the pooled solution with nitrogen gas was performed with a nitrogen evaporator (N-EVAP112, Organomation, USA). Dried pellets were dissolved in Acetonitrile: Ammonium/Acetate (4:6). An Agilent 1200 series liquid chromatography system (Waldbronn, Germany) equipped an ZORBAX Eclipse Plus C8 Narrow Bore guard column (Agilent, USA), and an ZORBAX

Eclipse Plus C8 Narrow Bore column (Agilent, USA) was used for chromatographic separation. For tandem mass spectrometry, Agilent 6410B triple quadrupole mass spectrometer with Agilent Masshunter Workstation was used.

2.2.3 Immunostaining of c-Fos in the brain slices

Adult 6 week-old male CD-1 mice were first habituated to the oral garage treatment for a period of ten days. The control and PFOS-treated groups were subjected to the same handling, habituation, and experimental procedures.Then the animals were subjected to oral garage treatment of PFOS (1 mg/kg or 5 mg/kg PFOS in corn oil) or corn oil alone as a control. Three hours later, mice were transcardially perfused with 4% Paraformaldehyde fix Solution (AR1068, BOSTER, China) while under deep anesthesia. The brain was harvested and postfixed in 4% PFA for one day. Following cryoprotection in PBS with 30% sucrose for two days, the brains were cut into 30 μm slices with a cryostat. Then, brain sections were incubated with primary antibodies (rabbit anti-c-Fos; 1:500; 2250, Cell Signaling Technology, USA) for 12 hours at 4°C. Sections were incubated for 2 hours in secondary antibodies (Alexa Fluor Plus 488; A32731, Thermo Fisher, USA), then sections were incubated for 10 min with DAPI (4',6-diamidino-2-phenylindole, 0.4 μg/mL, Sigma, USA). Images were captured by VS120 Virtual Slide Microscope (Olympus, Japan). PFOS activation was quantified by cell counting in brain nuclei with obvious c-Fos signals.

2.2.4 Open field test (OFT) and behavioral analysis

A white polyvinyl chloride open field (50 cm x 50 cm) with a black bottom was used to measure both the locomotion and anxiety-like behavior of the animals. The animal activity in the open field for 15 min was recorded and then analyzed. Total distance, average speed, time in the center, entries to the center were analyzed using anymaze (Stoelting, USA). Between mice, the apparatuses were cleaned with an ethanol solution of 20%.

2.2.5 Sample preparation and untargeted metabolomic analysis

At the end of the 21-day treatment, hypothalamus tissue was sectioned out from the fresh brain using mouse Brain Matrices (RWD, Shenzhen, China) and stored at -80°C before use. Frozen brain tissue was thawed on ice and homogenized with 120 μL of precooled 50% methanol buffer, then the mixture was vortexed for 1 min and incubated for 10 min at 25℃. The supernatant was transferred into 96-well plates after centrifugation at 4,000 g for 20 minutes. A TripleTOF® 5600+ System (SCIEX, USA) was used for analysis of all samples in both positive and negative ion modes. The ultra-performance liquid chromatography (UPLC) system (SCIEX, UK) was used for chromatographic separation. Reversed-phase separation was performed using an ACQUITY UPLC T3 column (100 mm*2.1 mm, 1.8 μm, Waters, UK). It was introduced for the separation of metabolites that the mobile phase consisted of solvent A (water, 0.1% formic acid) and solvent B (Acetonitrile, 0.1% formic acid). The gradient elution conditions were as follows with a flow rate of 0.4 mL/min: 5% solvent B for 0-0.5 min; 5-100% solvent B for 0.5-7 min; 100% solvent B for 7-8 min; 100-5% solvent B for 8-8.1min; and 5% solvent B for 8.1-10min. The column temperature was maintained at 35℃. The curtain gas pressure was set to 30 PSI, while the ion source gas1 and gas2 pressures were set to 60 pounds per square inch . Temperature of the interface heater was 650 °C. The ion spray floating voltage was set at 5 kV for the positive-ion mode, and -4.5 kV for the negative-ion mode. A data-independent acquisition mode was used to acquire the MS data. When the threshold of 100 counts/s was exceeded with a 1+ charge state, survey scans were collected every 150 ms and up to 12 product ion scans were collected. The mass range of 60-1200 Dalton. The total cycle time was fixed at 0.56 s. Four-time bins were summed for each scan at a pulse frequency of 11 kHz by monitoring the 40 GHz multichannel TDC detector with four-anode/channel detection. Dynamic exclusion was set for 4 s. The mass accuracy was calibrated every 20 samples during the entire acquisition period. The stability of the LC-MS was also tested by analysing a quality control sample every ten samples. Each ion was identified by the comprehensive information of retention time and mass-to-charge ratio (M/Z). The three-dimensional matrix containing arbitrarily assigned peak indices (retention time-m/z pairs), sample names (observations), and ion intensity information (variables) were matched to the in-house and public database. Annotation of metabolites was

conducted by matching the M/Z to those in the Encyclopedia of Genes and Genomes (KEGG) and HMDB (Human Metabolome Database) within a 10 ppm threshold. Metabolites detected in less than 50% of QC samples or 80% of tested samples were removed. The k-nearest neighbor algorithm was used for the improvement of missing peaks. The group datasets were normalized using a probabilistic quotient normalization algorithm. QC-robust spline batch correction was performed using QC samples. The P-value analyzed by student t-tests was used for the different metabolite selections. The differential metabolites were selected with Fold change > 1.2 or < 0.5 and P-value < 0.05. MetaboAnalyst 5.0 was used for PCA and pathway analysis [118], and MBrole2.0 was sued for enrichment analysis [119].

2.2.6 Statistical Analysis

Results were presented as the Mean ± SEM. N refers to the number of mice used in each experiment. Statistical analyses were carried out using PRISM 8.0 (GraphPad Software Inc, USA). One way analysis of variance (ANOVA) followed by Tukey's multiple comparisons test or a student t-test was used and indicated in the figure legends respectively.

2.3 Results

2.3.1 PFOS treatment caused strong activation of the brain nuclei including LS, PVT and LC

Considering the capacity of PFOS to disrupt BBB and the vital role the brain plays in reproductive function, we want to know whether PFOS treatment causes any neuronal activation, especially in the hypothalamus. Adult CD-1 male mice were subjected to 1 mg/kg, 5 mg/kg PFOS or corn oil oral garage treatment. After three hours of oral gavage treatment, the brain was dehydrated and sectioned for c-Fos immunostaining. As a neuronal activity marker, c-Fos is involved in the signal transduction cascade that relates extracellular stimuli to intracellular events and can be used for neuronal activation detection. Our results showed that 5 mg/kg PFOS exposure significantly induced c-Fos expression in several brain regions,

including lateral septal nucleus (LS), paraventricular thalamic nucleus (PVT), and locus coeruleus (LC) (Fig 2.1, A-D). Quantitative analysis of c-Fos-positive signals at each brain nuclei revealed that 5 mg/kg PFOS significantly activated neurons in the lateral septal nucleus (LS), paraventricular thalamic nucleus (PVT), and locus coeruleus (LC) compared with the oil control (Fig 2.1, E). In contrast, there was no significant c-Fos expression in hypothalamic nuclei after PFOS exposure, including the medial preoptic area (mPOA), paraventricular nucleus (PVN), dorsomedial hypothalamic nucleus (DM), and ventromedial nucleus (VMH) (Fig 2.2, A-E).

2.3.2 PFOS was detected in the hypothalamus and altered the hypothalamic metabolome.

LC-MS/MS analysis showed that PFOS indeed entered the hypothalamus after 21-day treatment with a high concentration of 12,473 ng/mL PFOS from the hypothalamus of 5 mg/kg PFOS group; 1,467 ng/mL PFOS from the hypothalamus of 1 mg/kg PFOS group; while no detectable PFOS was found in the hypothalamus of the oil control group (Fig 2.3, A). It is noted that some cells do not express c-Fos when they are activated. It has been reported that cerebral metabolome was disturbed by perfluorooctanoic acid (PFOA), another member of the perfluoroalkyl substances family [113]. Therefore, we want to know whether the hypothalamic metabolome was altered by 1 and 5 mg/kg PFOS exposure. After 21-day PFOS exposure, the hypothalamus was harvested and subjected to metabolomic analysis. First, the Principal Component Analysis (PCA) analysis revealed two distinct clusters of the oil control group and the PFOS-treated groups (Fig 2.3, B). A heatmap plotting the differential metabolites among the three groups showed a consistent pattern (Fig 2.3, C). Among all the altered metabolites, several metabolites related to hypothalamic neurotransmitters and neuromodulators were found, including N-Docosahexaenoyl GABA, DL-glutamate, N-oleoyl GABA, N-palmitoyl GABA, D-pyroglutamic acid, L-tyrosine, and tryptophan (Fig 2.3, C). KEGG analysis showed that 1 and 5 mg/kg PFOS caused similar effects (Fig 2.4, A-B). Thus, common differential metabolites in the 1 mg/kg PFOS and 5 mg/kg PFOS group were subjected to metabolites set enrichment analysis. Results showed PFOS altered the ATP-binding cassette (ABC) transporters,

aminoacyl-tRNA biosynthesis, alanine, aspartate, and glutamate metabolism, phenylalanine metabolism, phenylalanine, tyrosine and tryptophan biosynthesis, glycine, serine and threonine metabolism and D-glutamine and D-glutamate metabolism (Fig 2.4, C; Table 2.1). Our results showed that PFOS could enter the hypothalamus and disturb hypothalamic metabolome, including those related to the hypothalamic neurotransmitters (glutamate and GABA) and neuromodulators (serotonin and dopamine).

2.3.3 PFOS treatment at 1 mg/kg and 5 mg/kg caused anxiety-liked behavior.

At the end of 21-day PFOS treatment, animals were subjected to an open field behavioral test (Fig 2.5, A-B). Our results showed that the locomotion of the mice was not significantly affected by the PFOS treatment as no significant change was found in the total distance and average speed in the apparatus (Fig 2.5, C-D). PFOS at 1mg/kg and 5mg/kg both induced anxiety-like behavior with significant reductions in the time spent in the center and a decreased tendency to enter the center (Fig 2.5, E-F). All three nuclei were previously demonstrated to be involved in anxiety circuitry, which might partly explain the anxiety-like behaviors in animals. [120-123]. Herein, we reported that PFOS treatment also causes anxiety-like behavior in male adult animals.

2.4 Discussion

The neurotoxic effects of 1 mg/kg and 5 mg/kg PFOS exposure were studied using c-Fos immunostaining, metabolomic analysis and behavioral analysis. Results showed 5 mg/kg PFOS caused anxiety-like behavior in the mice, and activated neurons within the lateral septum (LS), paraventricular nucleus of the thalamus (PVT), and locus coeruleus (LC). A high concentration of PFOS was detected in the hypothalamus. Disrupted hypothalamic metabolome was revealed using metabolomic analysis.

Adverse effects of PFOS on locomotion have been reported [114,124]. In this study, the total distance in both the 1 and 5 mg/kg groups was less than that in the control group. Interestingly, our results showed PFOS increased the anxiety-like behaviors of the mice, with decreased time in the center and entries to the center. In line with behavior test results, c-Fos immunostaining

revealed strong neuronal activation in three nuclei, LS, PVT, and LC. It has been reported that these three nuclei are involved in anxiety circuitry [120-123].

It has been reported that PFOS can enter the brain and cause adverse effects, but the underlying mechanism and its nuclei targets remain unclear. The neurotoxicity studies about mammalian PFOS exposure were limited [23,125]. Most of the neurotoxicity studies about PFOS use *C. elegans* or *Planaria* [93,126], zebrafish [115], or cell lines [127-130]. LC-MS/MS analysis proved PFOS existence in the brain with a high concentration of 12,473 ± 2,906 ng/g in the 5 mg/kg group. However, no strong c-Fos activation in the hypothalamic nuclei was found after acute PFOS treatment. Next, the metabolomic analysis of the hypothalamic tissue was carried out. Metabolites set enrichment analysis revealed PFOS disrupted aminoacyl-tRNA biosynthesis, ATP-binding cassette (ABC) transporters, glycine, serine and threonine metabolism, and pathways related to neurotransmitters or neuromodulators, including Alanine, aspartate and glutamate metabolism, D-glutamine and D-glutamate metabolism and phenylalanine, tyrosine, and tryptophan biosynthesis. It has been reported that PFOA altered BALBc cerebral metabolomics [131]. Interestingly, PFOA exposure caused altered metabolic pathways including glutathione, glycerophospholipid, arginine, proline, tyrosine, histidine, tryptophan, alanine, aspartate, glutamate and D-glutamine and D-glutamate. Our data suggested that PFOS altered the hypothalamic amino acid metabolism (i.e., arginine, histidine, D-glutamine, D-glutamate, alanine, aspartate, glutamate and phenylalanine, tyrosine, and tryptophan). As a result, it is indicated that cerebral amino acid metabolism and biosynthesis are the targets of PFOA and PFOS. Aminoacyl-tRNA synthetases (AaRSs) are ancient ubiquitously expressed housekeeping enzymes including in the brain that ensure faithful translation of genetic information into functional proteins [132]. Altered aminoacyl-tRNA biosynthesis pathway in the brain has been reported after ethanol ingestion [133], methylmercury exposure [134] and rabies virus infection [135]. Associations between faults in AaRS-mediated processes and human diseases have been recognized including the pathology of the human nervous system like epilepsy, developmental delay, and cerebellar atrophy [132]. The aminoacyl-tRNA biosynthesis pathway implies possible brain functional disturbance by PFOS exposure including the elevated anxiety-like behavior and decreased male fecundity we already observed. It is not surprising to find that

PFOS exposure alters the ABC transporters pathway. The ATP-binding cassette (ABC) gene family is highly expressed in the brain endothelial cells and plays an important role in brain homeostasis by protecting the brain from potentially harmful endogenous and exogenous substances [136,137]. Functionally, ABC transporter acts as efflux pumps and prevents harmful compounds from crossing the tight junction, dysfunction of which have been implicated in neurodegenerative diseases, including Alzheimer's disease [138], Parkinson's disease [139], and epilepsy [140]. Disturbed amino acids glycine, serine and threonine metabolism pathway was previously reported to be related to brain diseases including major depression [141], attention deficit hyperactivity disorder (ADHD) and anxiety [142]. Disturbed pathways related to neurotransmitters or neuromodulators suggest that PFOS exposure might interfere with the local hypothalamic neural activity and its signals.

2.5 Summary

In this study, we found that PFOS crossed the blood-brain barrier, disrupted mice's hypothalamic metabolic profiles, and caused anxiety-like behavior. LC-MS/MS analysis showed the presence of PFOS in the hypothalamus. Immunostaining of c-Fos showed anxiety-related nuclei were activated, including LS, PVT, and LC. Open field test suggested PFOS caused anxiety-like behavior in mice with no significant impact on locomotion. Metabolomic analysis revealed the altered pathway for aminoacyl-tRNA biosynthesis, ABC transporters, neurotransmitters or neuromodulators. The disruption of metabolic pathways in the brain may cause damage to the blood-brain barrier, increase the incidence of neurodegenerative disorders, and interfere with the hypothalamic regulation mechanism.

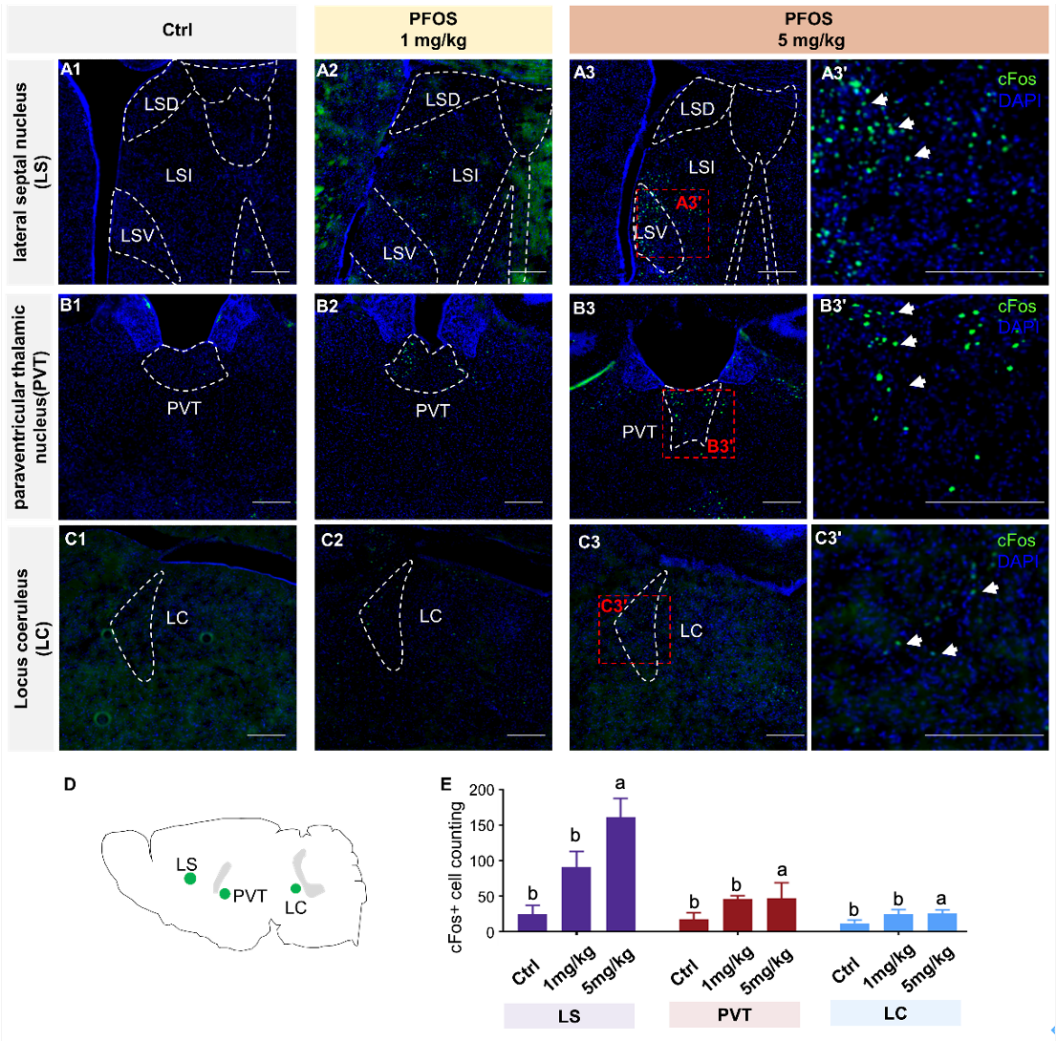

Fig 2.1 PFOS treatment caused strong activation of brain nuclei LS, PVT and LC.

(A1, B1, C1) The oil control group showed no significant c-Fos activation in the brain. (A2, B2, C2); PFOS exposure at the dose of 1 mg/kg resulted in activation of the cells in the LS, PVT, and LC. (A3, B3, C3); PFOS exposure at the dose of 5 mg/kg caused strong activation of the cells in the LS, PVT, and LC, with enlarged pictures at the right in A3', B3', C3' demonstrating the c-Fos positive staining; green, c-Fos immunostaining, blue, DAPI; scale bars = 200 μm; arrows, c-Fos positive staining; LS, lateral septal nucleus; PVT, paraventricular thalamic nucleus; LC, locus coeruleus. (D-E) Quantification of c-Fos-positive cells showed 5 mg/kg PFOS treatment caused a significant increase of neuron activation in the LS, PVT, and LC compared with oil control; data were presented as mean ± SEM, n = 3 for each group; different letters above the bar charts were significantly different according to the results of one-way ANOVA with Tukey's test ($P<0.05$).

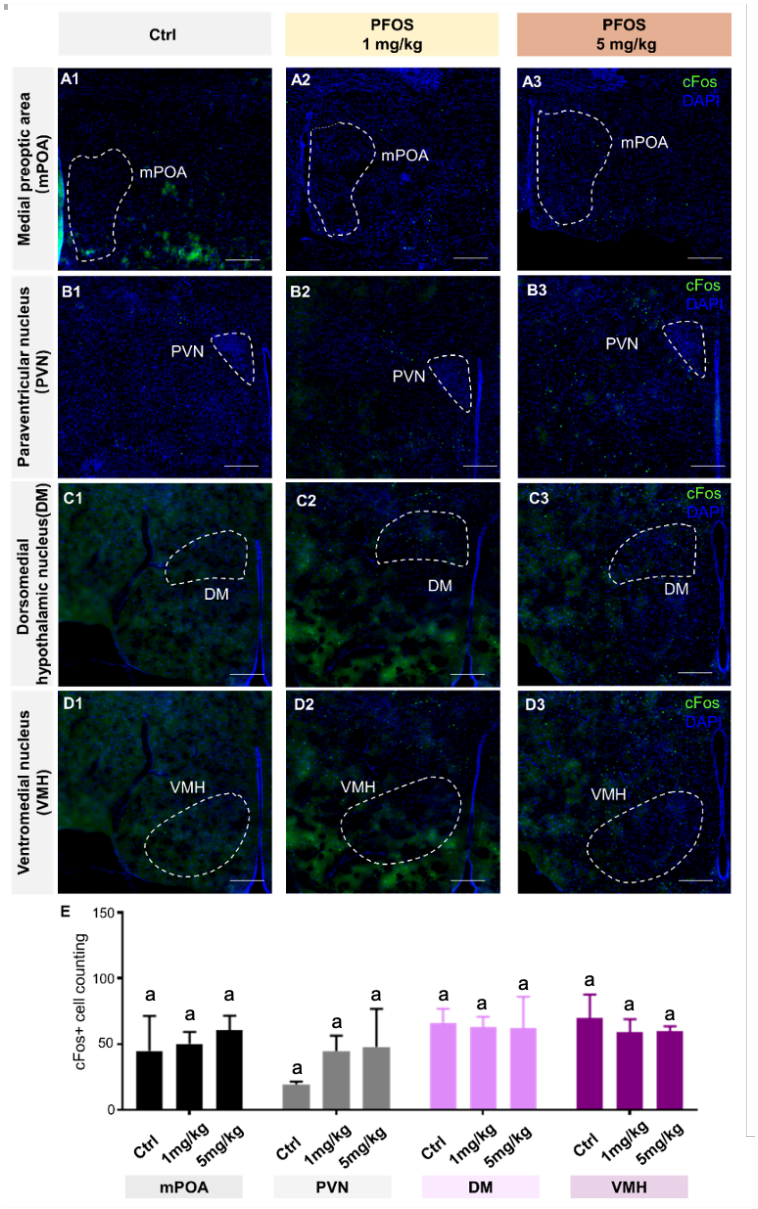

Fig 2.2 PFOS treatment caused no significant activation of the hypothalamus.

(A-D) PFOS treatment at 1 mg/kg and 5 mg/kg caused no significant activation of neurons in the hypothalamic nuclei, including mPOA, PVN, DM, and VMH. Green, c-Fos immunostaining, blue, DAPI; scale bars = 200 μm; mPOA, medial preoptic area; PVN, paraventricular nucleus; DM, dorsomedial hypothalamic nucleus; VMH, ventromedial nucleus. (E) Quantification of c-Fos-positive cells showed PFOS treatment caused no significant increase of neuron activation in the MPOA, PVN, DM, and VMH compared with oil control; data were presented as mean ± SEM, n = 3 for each group; different letters above the bar charts were significantly different according to the results of one-way ANOVA with Tukey's test (<0.05).

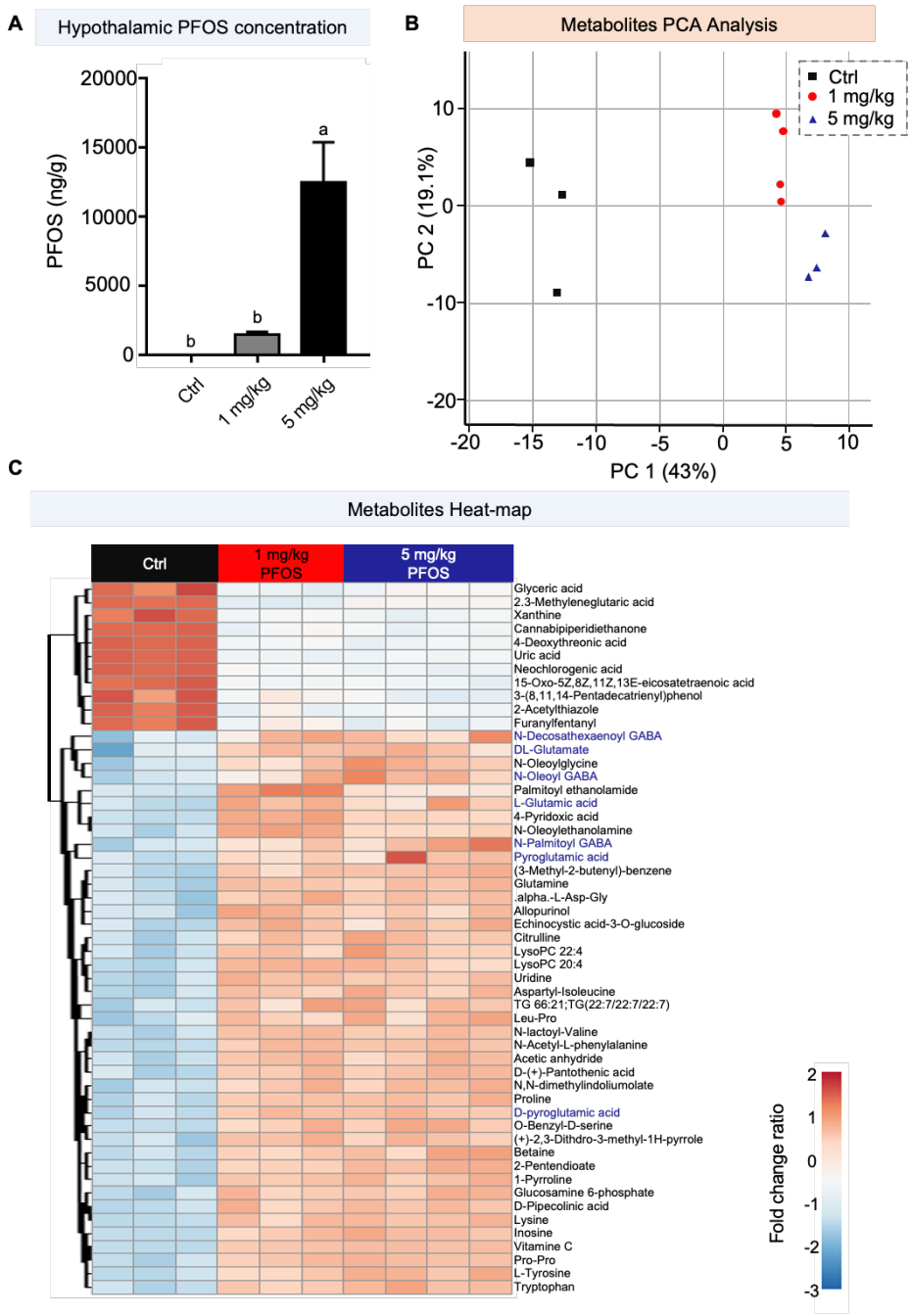

Fig 2.3 PFOS treatment altered the hypothalamic metabolome.

(A) PFOS was detected in the hypothalamus at the end of 21-day treatment; data were presented as mean ± SEM, n = 3 per group; different letters above the bar charts were significantly different according to the results of one-way ANOVA with Tukey's test ($P<0.05$). (B) Principal Component Analysis of the metabolites detected in three groups. (C) Heatmap of differential metabolites among three groups. n = 3 for the control group; n = 3 for the 1 mg/kg group; n = 4 for the 5 mg/kg group.

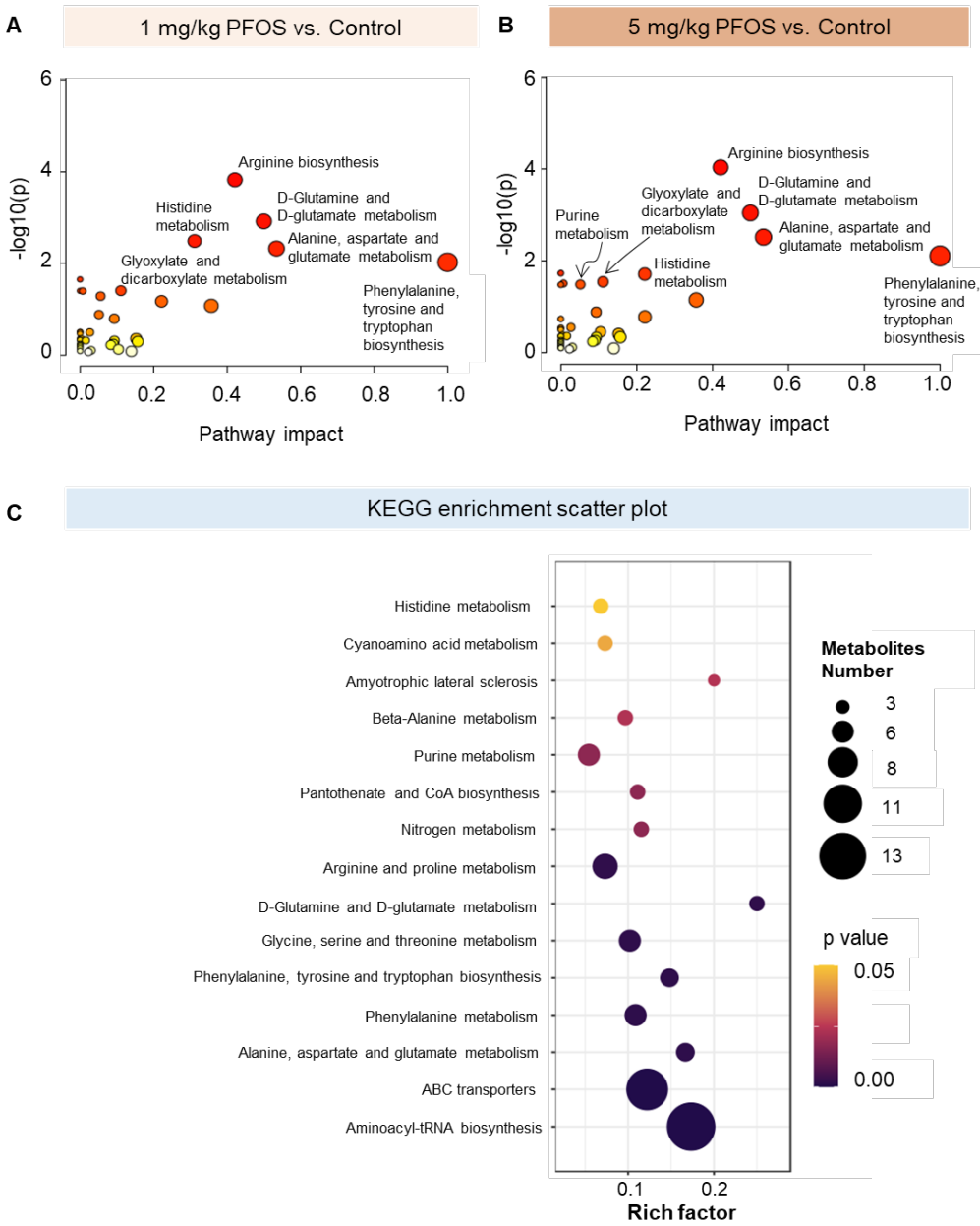

Fig 2.4 KEGG analysis revealed key pathways affected in the hypothalamus by PFOS treatment.

(A-B) Altered metabolites pathways by 1 mg/kg PFOS or 5 mg/kg PFOS compared with control. (C) KEGG enrichment analysis based on common altered metabolites caused by 1 mg/kg PFOS and 5 mg/kg PFOS treatment; n = 3 for control group; n = 3 for 1 mg/kg group; n = 4 for 5 mg/kg group.

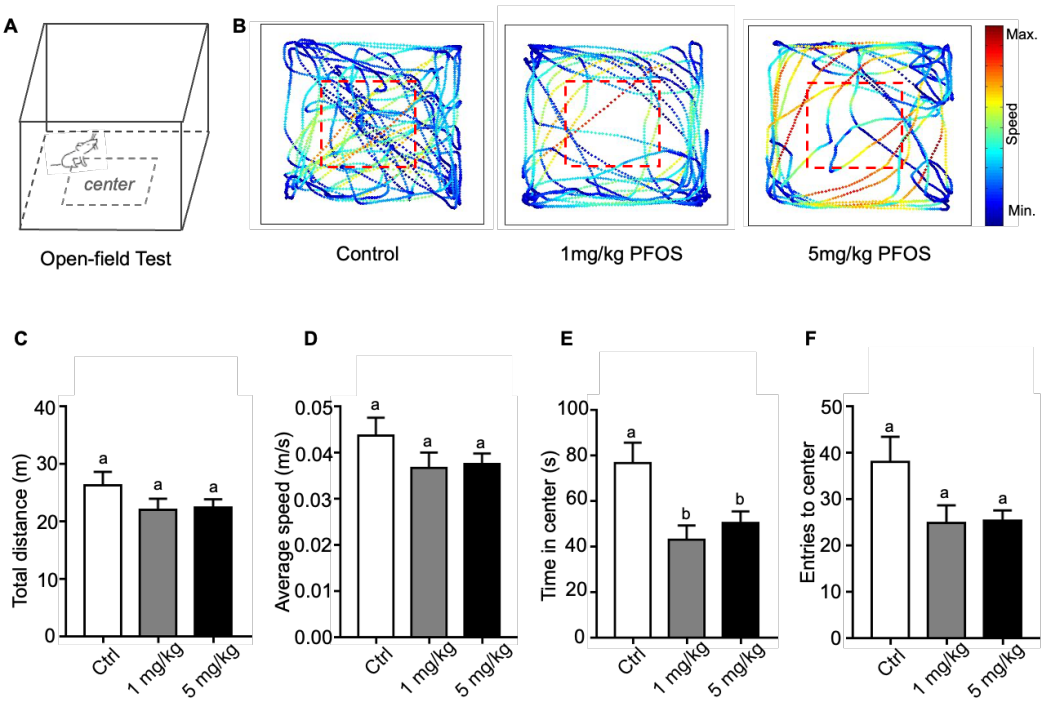

Fig 2.5 PFOS treatment caused anxiety-like behavior.

(A) The Open-field test paradigm was used to assess the animal's anxiety-like behavior. (B) The representative track plot of the tested mice from the control and PFOS treated groups. (C-D) The locomotion of the mice was not significantly affected by the PFOS treatment as reflected by the total distance and average speed in the open-field. (E-F) PFOS at 1mg/kg and 5mg/kg both caused anxiety-like behavior in the mice for a significant decrease in the time in center and a trend in entries to center parameters; data were presented as mean ± SEM, n = 9 per group; different letters above the bar charts were significantly different according to the results of one-way ANOVA with Tukey's test ($P<0.05$).

Table 2.1 PFOS altered hypothalamic metabolic pathways.

Annotation	FDR	Metabolites
Aminoacyl-tRNA biosynthesis	2.36636E-11	L-Glutamic acid, L-Lysine, L-Aspartic acid, L-Arginine, L-Glutamine, L-Methionine, L-Tryptophan, L-Phenylalanine, L-Methionine, L-Tryptophan, L-Phenylalanine, L-Tyrosine, L-Histidine, L-Proline L-Valine, L-Threonine
ABC transporters	5.23467E-08	L-Glutamic acid, L-Lysine, L-Aspartic acid, L-Arginine, L-Glutamine, L-Phenylalanine, L-Histidine, L-Proline, L-Valine, L-Threonine, Betaine
Alanine, aspartate and glutamate metabolism	0.001601069	L-Glutamic acid, L-Aspartic acid, L-Glutamine, Glucosamine 6-phosphate
Phenylalanine metabolism	0.001601069	L-Phenylalanine, L-Tyrosine, 2-Hydroxycinnamic acid, 2-Phenylacetamide, N-Acetyl-L-phenylalanine
Glycine, serine and threonine metabolism	0.001691579	L-Aspartic acid, L-Tryptophan, L-Threonine, Glyceric acid, Betaine
Phenylalanine, tyrosine and tryptophan biosynthesis	0.001691579	L-Tryptophan, L-Phenylalanine, L-Tyrosine, Indole
Arginine and proline metabolism	0.001791874	L-Glutamic acid, L-Aspartic acid, L-Arginine, L-Proline, Citrulline
D-Glutamine and D-glutamate metabolism	0.001791874	L-Glutamic acid, L-Aspartic acid, L-Glutamine

Chapter 3 PFOS affects sperm quality by reducing epididymal sperm motility

3.1 Introduction

Perfluorooctanesulfonic acid (PFOS) is a fully fluorinated chemical and is highly persistent in the environment. Since 1949, PFOS has been used in paper coating, stain- and water-repellent fabrics, wetting agents, nonstick coating of cookware, and aqueous film-forming foam (AFFF) [7]. The high stability of PFOS makes it difficult to degrade naturally, and extensive consumption contributes to its widespread distribution in the environment. The residual PFOS in the ocean is estimated to be approximately 1,000 tons [143]. Liu et al. systematically analyzed the PFOS emission in mainland China and estimated that approximately 85% of PFOS comes from industrial wastewater discharge, the rest comes from landfill leachate and AFFF application [144]. Zhou et al. conducted an assessment of PFAS exposure in fishery employees in the capital of Hubei [19]. The results showed abnormally high levels of PFOS in piscatory serum (9,260 - 31,400 ng/ml) compared to background individuals.

Animal studies have shown PFOS causes hepatotoxicity, neurotoxicity, reproductive toxicity, and immunotoxicity in mice, rats, zebrafish or cell lines [145]. PFOS can act as hormonally active agents to interfere with androgen or estrogen synthesis, secretion, transport, binding [145]. It was reported that exposure to PFOS decreased testes weight and reduced total sperm count due to apoptosis of germ cells [77]. Previous works have reported that PFOS disrupted cytoskeleton signaling, cell-cell junction of Sertoli cells, and perturbed the blood-testis barrier (BTB) [79-81]. The direct effects of PFOS on Leydig cells were revealed through a CREB/CRTC2/StAR signaling pathway [146]. These results suggested that PFOS can interrupt spermatogenesis and steroidogenesis. Toft et al. reported negative associations between PFOS exposure and sperm morphology [147]. Song et al. reported negative correlations between sperm progressive motility and semen PFASs levels in south China [148]. Nevertheless, Raymef et al. indicated no significant association among sperm concentration, sperm motility, and PFOS levels in serum [149]. It is noted that reproductive functions are under the control of the hypothalamic-pituitary-gonadal

(HPG) axis. Most of the studies so far have focused on the effects of PFOS on the testis or ovary. However, there are less data about the effects of PFOS on the HPG axis. In chapter two, we found that PFOS altered several metabolites levels related to glutamine, glutamine, tyrosine, and tryptophan, all of which are involved in the regulation of pulsatile GnRH secretion. Therefore, we further investigated the testicular function after 21-day PFOS oral gavage treatment through sperm quality analysis, serum reproductive hormone levels determination, and testicular transcriptome analysis. Results showed that PFOS exposure altered serum LH levels and the testicular transcriptome, which caused impaired sperm quality.

3.2 Material and Methods

3.2.1 Animals

6 week-old male CD-1 mice (Zhejiang Vital River Laboratory Animal Technology Co., Ltd) were gouped-housed with 12:12-h light/dark cycle. The animals were fed with food pellets and water ad libitum. All husbandry and experimental procedures in this study were approved by the Animal Care and Use Committee of the Shenzhen Institute of Advanced Technology, Chinese Academy of Sciences, China. The mice were randomly divided into three groups (10~15 individuals per group). Perfluorooctanesulfonate acid (PFOS, 98% purity, Shanghai ZZBIO Co., Ltd, China) was dissolved in dimethyl sulfoxide (D5879-1L, Sigma, USA) prior to mixing with corn oil (C7030, Solabio, China). The mice were weighed and orally administered 1 or 5 mg/kg PFOS in corn oil by gavage daily in the morning for 21 days. Body weight was recorded every other day. On day 21, the animals were anesthetized with pentobarbital 50mg/kg intraperitoneally. Caudal epididymis was used for sperm activity examination. After collecting blood through cardiocentesis and centrifuging it at 3000 x g, serum was collected and stored at -80°C for further analysis.

3.2.2 LC-MS/MS analysis of PFOS concentrations

After the 21-day treatment, blood, epididymis, and brain tissues were subjected to PFOS content analysis by LC-MS/MS. Briefly, tissues were mixed with internal standard (PFOS,

purity > 98%, MPFACMXA0714, Wellington Laboratories, Canada), 0.5 M TBA, and 0.25 M sodium carbonate buffer. Then, the mixture was placed in an orbital shaker at 250 rpm for 20 min. After centrifugation at 3000 rpm for 15 minutes, the organic layer was transferred to a new tube. All of the organic fractions were pooled after repeated extractions. Drying the pooled solution with nitrogen gas was performed with a nitrogen evaporator (N-EVAP112, Organomation, USA). Dried pellets were dissolved in Acetonitrile: Ammonium/Acetate (4:6). An Agilent 1200 series liquid chromatography system (Waldbronn, Germany) equipped an ZORBAX Eclipse Plus C8 Narrow Bore guard column (Agilent, USA), and an ZORBAX Eclipse Plus C8 Narrow Bore column (Agilent, USA) was used for chromatographic separation. For tandem mass spectrometry, an Agilent 6410B triple quadrupole mass spectrometer with Agilent Masshunter Workstation was used.

3.2.3 Sperm motility analysis

Sperm were collected from the caudal epididymis and suspended in HTF medium (M1130, Nanjing Aibei Biotechnology, China) for 10 min before being loaded and subjected to the computer-assisted sperm analysis (Beijing Suiplus, China). The CASA system includes a Nikon E200 microscope equipped with a Basler scout780-54fc area scan camera at 36 frames per second. Sperm count, motile sperm percentage, Curvilinear velocity (VCL), Straight-line velocity (VSL), Average path velocity (VAP) were analyzed to characterize sperm motility.

3.2.4 Reproductive hormone Analysis

At the end of the 21-day treatment, serum was used for testosterone, luteinizing hormone (LH), and follicle-stimulating hormone (FSH) levels determination using ELISA kits (testosterone, EM1850; FineTest, Wuhan, China. Range of 0.313-20 ng/ml; Sensitivity of 0.188 ng/ml; Intra-Assay CV<8%; Inter-Assay CV<10%; FSH, EM1035; FineTest, Wuhan, China. Range of 2.344-150 mIU/ml; Sensitivity of 1.406mIU/ml; Intra-Assay CV<8%; Inter-Assay CV<10%; LH, EM1188, FineTest, Wuhan, China. Range of 0.369-30 ng/ml; Sensitivity of 1.406mIU/ml; Intra-Assay CV<8%; Inter-Assay CV<10%). The assays were carried out following the manufacturer's protocols.

3.2.5 Sample preparation and RNA-seq analysis

At the end of the 21-day treatment, testes tissue was collected and stored at -80°C. Total RNA was extracted using Trizol reagent (15596018, Thermo Fisher, USA) following the manufacturer's procedure. After extraction, Dynabeads Oligo (dT) (Thermo Fisher, USA) was used for mRNA purification from total RNA (5μg). Following purification, , the mRNA was fragmented using divalent cations under 94°C for 5-7 minutes. SuperScript™ II Reverse Transcriptase (1896649, Invitrogen, USA) was used for cDNA reverse transcription, then *E. coli* DNA polymerase I (M0209, NEB, USA), RNase H (M0297, NEB, USA), and dUTP Solution (R0133, Thermo Fisher, USA) were used for U-labeled second-stranded DNA synthesis. A-base was then added to the blunt ends of each strand, preparing them for ligation to the indexed adapters. Each adapter contained a T-base overhang for ligating the adapter to the A-tailed fragmented DNA. Dual-index adapters were ligated to the fragments, and size selection was performed with AMPure XP beads. After the heat-labile UDG enzyme (M0280, NEB, USA) treatment of the U-labeled second-stranded DNAs, the ligated products were amplified with PCR. The average insert size for the final cDNA libraries was 300 ± 50 bp. The 2 × 150 bp paired-end sequencing on an Illumina Novaseq™ 6000 (LC-Bio Technology, China). The differentially expressed genes (DEGs) were selected with |log 2 fold change| ≥ 0.3 and q value < 0.05 using DESeq2. Then, DEGs were subjected to Gene Ontology (GO) enrichment analysis.

3.2.6 Quantitative real-time PCR (qPCR) analysis

Testes tissues were homogenized in 1 mL Trizol (15596026, Thermo Fisher, USA) and placed at Room temperature for 5 min. Add 200 μL chloroform (AR500ML, SRC, China) and vortex for 10 sec. The mixture stands for 5 min at room temperature. Then, centrifuge at 12,000 rpm for 15 min at 4°C. The upper clean phase is transferred to a fresh 1 mL tube with the same volume of isopropanol (AR500ML, Dongjiang, China), and vortex for 10 sec. The mixture stands for 10 min at room temperature. Then, centrifuge at 12,000 rpm for 15 min at 4°C. Remove all supernatant. Precipitate RNA pellet in 1 mL 75% ethanol. Then centrifuge at 7,500

rpm for 10 min at 4°C. Retain the RNA pellet and remove all supernatant. Let stand for 20 min at Room temperature and then add 50 μL Rnase-free ddH2O. 1 μg purified RNA is used for reverse transcription PCR using ReverTra AceTM qPCR RT Kit (FSQ-101, TOYOBO, Japan) according to the manufacturer's protocol. The reactions were incubated at 37°C for 15 min, followed by 98°C for 5 min. After reactions, place the sample on ice for 10 min. Then dilute cDNA with 200 μL ddH_2O. Quantitative real-time PCR (qPCR) is conducted using the SYBR Green Master Mix (TOYOBO QPK-201, China). Reaction included 4.6 μL cDNA, 0.2 μL of each primer (10 μM), and 5 ul SYBR Green Master mix. The reactions were incubated in the 96-well PCR plates (HSR9905, BIO-RAD, USA) at 95°C for 10 min, followed by 40 cycles at 95°C for 15 sec and 60°C for 1 min. Reactions were run in triplicate. The relative fold gene expression of samples is calculated with the $2^{-\Delta\Delta Ct}$ method

Table 3.1 List of qPCR primers

Gene	forward primer sequence	reverse primer sequence
Gapdh	AGGTCGGTGTGAACGGATTTG	TGTAGACCATGTAGTTGAGGTCA
Dnaic2	CATCGACATCTTACCCAACCC	CTCGTGTTCCGACATACTGGC
Rimbp3	TCATTCTCCAAACGACCTGCT	GGCCCTTACCTCGGATTCA
Nup210l	CAACAAACTCAATGTGCCTCAAG	TGGAATGCCAGATGTAGCAGC
Dync1h1	GGGATGAGTATGCCACGCTG	TGTCCTTGAGCCCCTCTGAG
Dnahc10	CTCACCAACCCTATGCTATTCG	GCACCAGTATGCGGTAGAAGA
Lhr	CGCCCGACTATCTCTCACCTA	GACAGATTGAGGAGGTTGTCAAA

3.2.7 Statistical analysis

Results were presented as the Mean ± SEM. N refers to the number of mice used in each experiment. Statistical analyses were carried out using PRISM 8.0 (GraphPad Software Inc, USA). One way analysis of variance (ANOVA) followed by Tukey's multiple comparisons test or a student t-test was used and indicated in the figure legends respectively.

3.3 Results

3.3.1 PFOS was detected in the circulation and epididymis

In this study, adult CD-1 male mice were subjected to 1 mg/kg, 5 mg/kg PFOS or corn oil oral gavage treatment daily for 21 days (workflow in Fig 3.1, A). The body weight of each mouse was recorded every other day. No mice died during the study. At the end of the treatment, serum and epididymides were used for PFOS levels determination. The three groups did not differ significantly in regards to bodyweight change following PFOS treatment (Fig 3.1, B). The PFOS concentrations in serum of the control group, the 1 mg/kg group, and the 5 mg/kg group were 12.42 ± 0.7037 ng/mL, 27,566 ± 1,657 ng/mL, and 248,921 ± 31,607 ng/mL, respectively (Fig 3.1, C). High PFOS levels were detected in the epididymis in the 1 and 5 mg/kg groups with 1,600 ± 361.2 ng/g and 7,423 ± 2,110 ng/g, respectively.

3.3.2 PFOS treatment at 1 mg/kg and 5 mg/kg both resulted in reduced sperm motility.

At the end of the 21-day PFOS treatment, we determined the effects of PFOS on testicular functions. First, we determined the serum reproductive hormone levels using ELISA kits. Results showed both 1 and 5 mg/kg PFOS exposure led to a downward trend in testosterone levels though not significant, which was in agreement with the previous study (Fig 3.2 A,a) [76]. 5 mg/kg PFOS exposure significantly reduced serum LH levels (Fig 3.2 A,b), while no significant difference was found in FSH levels (Fig 3.2 A,c). Then computer-assisted sperm analysis (CASA) was used for epididymal sperm quality qualification among the three groups. No significant difference was found in total sperm counting or the percentage of motile sperm among the three groups (Fig 3.2 B,a-b). Both 1 and 5 mg/kg PFOS treatment resulted in a significant decrease in Curvilinear Velocity (229.8 ± 7.139 μm/s in control group, 183.5 ± 15.92 μm/s in 1 mg/kg group, and 178 ± 5.903 μm/s in 5 mg/kg group) (Fig 3.2 B, c) and Average Path Velocity (108.6 ± 3.521 μm/s in control group, 90.97 ± 6.79 μm/s in 1 mg/kg group and

87.84 ± 2.912 μm/s in 5 mg/kg group) (Fig 2.2 B,d). As for Straight-line Velocity, 5 m/kg PFOS exposure led to a significant decrease (82.03 ± 5.293 μm/s in control group, 60.4 ± 3.891 μm/s in 5 mg/kg group) (Fig 3.2 B,e). There was a downward trend for the Straight-line Velocity (VSL) in 1 mg/kg group (64.72 ± 8.321 um/s in 1 mg/kg group, $p = 0.129$) (Fig 2.2 B,e). In summary, our results are consistent with our previous report that PFOS exposure decreased reproductive hormone (testosterone and LH levels) and reduced sperm motility.

3.3.3 PFOS treatment alter testicular transcriptome related to spermatogenesis and steroidogenesis.

Testicular transcriptome analysis between the control group and the 5 mg/kg PFOS treatment group revealed a total of 217 differentially expressed genes (DEGs), including 118 up-regulated and 99 down-regulated genes (Fig 3.3 A). These DEGs were then subjected to Gene Ontology (GO) enrichment analysis (Fig 3.3 B; Table 3.2). According to the Go enrichment analysis, PFOS caused alteration of motor activity, microtubule motor activity, microtubule-based movement, cytoskeleton, cilium movement, and spermatid development, which could account for the reduced sperm motility we observed (Fig 3.3 C). PFOS treatment also altered cholesterol biosynthetic and metabolic process, steroid metabolic process, and steroid biosynthetic process (Fig 3.3 C). For example, altered genes involved in spermatogenesis included *Dync1h1*, *Rimbp3*, *Dnaic2*, *Dnah10*, and *Nup210l*, all of which were down-regulated (Fig 3.4). The decreased gene expression was validated by quantitative real-time PCR (qPCR) (Fig 3.5). The decreased gene expression of the luteinizing hormone receptor (*Lhr*) after PFOS treatment, together with the decreased circulating LH levels (Fig 3.2 A,b), suggested PFOS disturbed the HPG axis and impaired sperm quality.

3.4 Discussion

The adverse impact of PFOS on reproductive function has been investigated. Epidemiologically, sperm progressive motility was negatively correlated to serum concentrations of PFOS ($p = 0.019$) [148]. The results of an investigation of the effects of PFOS exposure on sperm quality

in the Arctic and European populations indicated that PFOS affected endocrine activity or sperm membrane function [147]. It has been reported that prenatal or developmental exposure to PFOS impaired male reproductive function. Khezri et al. investigated the effects of maternal exposure to POPs mixtures on the reproductive function of male offspring and found that the POP-exposed animals suffered a decrease in sperm chromatin integrity and sperm production [150]. Lai et al. examined the effects of in utero PFOS exposure on offspring testicular function and found that the male offspring exhibited decreased serum testosterone and lower epididymal sperm counts [82]. Lessard et al. investigated the adverse effects of prenatal POPs mixture exposure on multiple generations of males from F1 to F4 and suggested POPs mixture significantly reduced sperm viability in F1, F2, and F3 generations with no significant effect on sperm motility parameters (VCL, VSL, and VAP) [151]. In our study, adult PFOS exposure caused epididymal sperm motility reduction with no significant impact on total sperm counts or sperm viability. The mechanism of reproductive toxicity of a mixture of POPs may not work in the same way as a single pollutant. Different exposure periods (prenatal phase, postnatal phase, adolescence, and adulthood) might result in different outcomes.

Previous studies have reported the effects of PFOS on Sertoli cells F-actin and microtubule organization [152]. An *in vitro* study showed rats Sertoli cells exhibited mislocalization of actin-related protein 3 and actin-bundling protein palladin, which caused actin microfilaments disruption and resulted in Sertoli cells injury after PFOS treatment [153]. Besides, PFOS treatment also caused the fragmentation of tight junction protein ZO-1 and disorganized distribution of basal ectoplasmic specification proteins N-cadherin and β-catenin in rat Sertoli cells [154]. These results implied PFOS perturbs the cytoskeleton of Sertoli cells by disorganizing microtubules and actin filaments of the cytoskeleton. As for spermatozoa, the precession relies on the wobbling flagellum or tail called axoneme (‘9+2’ structure, two central microtubules and nine outer doublet microtubules). Transcriptome results showed that the axoneme-related genes *Dnaic2* and *Dnah10* were down-regulated. GO enrichment showed that PFOS altered biological processes related to spermatid development. At the midpiece of sperm, there are large amounts of specialized mitochondria responsible for ATP generation. As a result, PFOS might disrupt sperm axoneme structure and reduce sperm precession ability. For example, transcriptome

results showed that PFOS down-regulated the myosin light chain kinase (*Mylk*) gene expression in rats Sertoli cells [154]. MYLK is a calmodulin (calm)-binding protein. Inhibition of MYLK by 1-(5-chloronaphthalene-1-sulfonyl)-1H-hexahydro-1,4-diazepine hydrochloride (ML-9) can reduce fowl spermatozoa motility [155].

Transcriptome analysis revealed that PFOS disrupted the structures of the axoneme and the manchette. Microtubule-based structure manchette only occurs during the spermatid elongation and surrounds the head of the spermatid and is responsible for sperm head shaping and development of the sperm neck and tail. Dysfunction of the manchette caused sperm morphological disorder [154]. Cytoplasmic dynein 1 heavy chain 1 (DYNC1H1) was encoded by *Dync1h1* belonging to the cytoplasmic dynein 1 complex [156]. It was found that *dynac1h1* knockdown rats failed to support spermatogenesis and spermiation due to disruption of the Sertoli cells microtubule organization [157]. Developing zebrafish exposed to 20 mg/L PFOS exhibited decreased *Dync1h1* mRNA levels and DYNC1H1 protein levels in the cilia organelle [158]. *Rimbp3* knockout mice exhibited infertility as their sperm showed abnormal heads, deformed nuclei, and uncoupled acrosomes [159]. Nucleoporin 210 like (NUP210L) protein encoded by *Nup210l* exclusively in the testis. Epidemiologically, Patients with homozygous loss of function of NUP210L suffered from decreased sperm count, reduced motility, and increased abnormal spermatozoa [160].

It is known that PFOS disordered lipid homeostasis and caused hypocholesterolemia [155,161,162]. In this study, transcriptome results suggested that PFSO disturbed long chain fatty acids biosynthesis. A survey conducted by Reiko Kishi and his colleagues showed a negative association between PFOS and maternal levels of triglycerides (TG) and several fatty acids including palmitic, palmitoleic, oleic, linoleic, α-linolenic, and arachidonic acids [163]. As for males, lipid homeostasis plays an important role in male reproductive function [164]. First, cholesterol is the precursor for steroids. Besides, there are abundant polyunsaturated fatty acids (PUFAs) on the sperm membrane, which are important for sperm viability and mobility [165]. PUFAs promote sperm membrane flexibility and fluidity [166,167]. For example, Docosahexaenoic Acid (DHA) is an n-3 polyunsaturated fatty acid and is supposed to improve sperm quality [168]. The sperm samples from asthenozoospermia patients who produce plenty of sperm with low

motility sperm showed lower PUFAs than normozoospermic sperm samples [169]. Martínez-Soto et al. found that DHA and other PUFAs contributed to sperm viability and motility parameters before and after the cryopreservation procedure [170]. It has been reported that prenatal PFOS exposure alters the mouse testis lipidome [82]. PFOS exposed mice exhibited a decreased level of DHA in the testis. There was less report concerning the effects of adulthood PFOS exposure on PUFAs levels. The disrupted fatty acid synthesis and metabolism caused by PFOS may alter spermatozoa lipid composition and impair sperm quality.

3.5 Summary

In this chapter, we reported that 21-day PFOS treatment disrupted the synthesis of luteinizing hormone, which has detrimental effects on testicular function. CASA results showed PFOS reduced caudal epididymal sperm motility with no significant difference in total sperm count. Transcriptome analysis showed that PFOS exposure altered the processes related to steroidogenesis, spermatogenesis, fatty acid synthesis, and lipid metabolism.

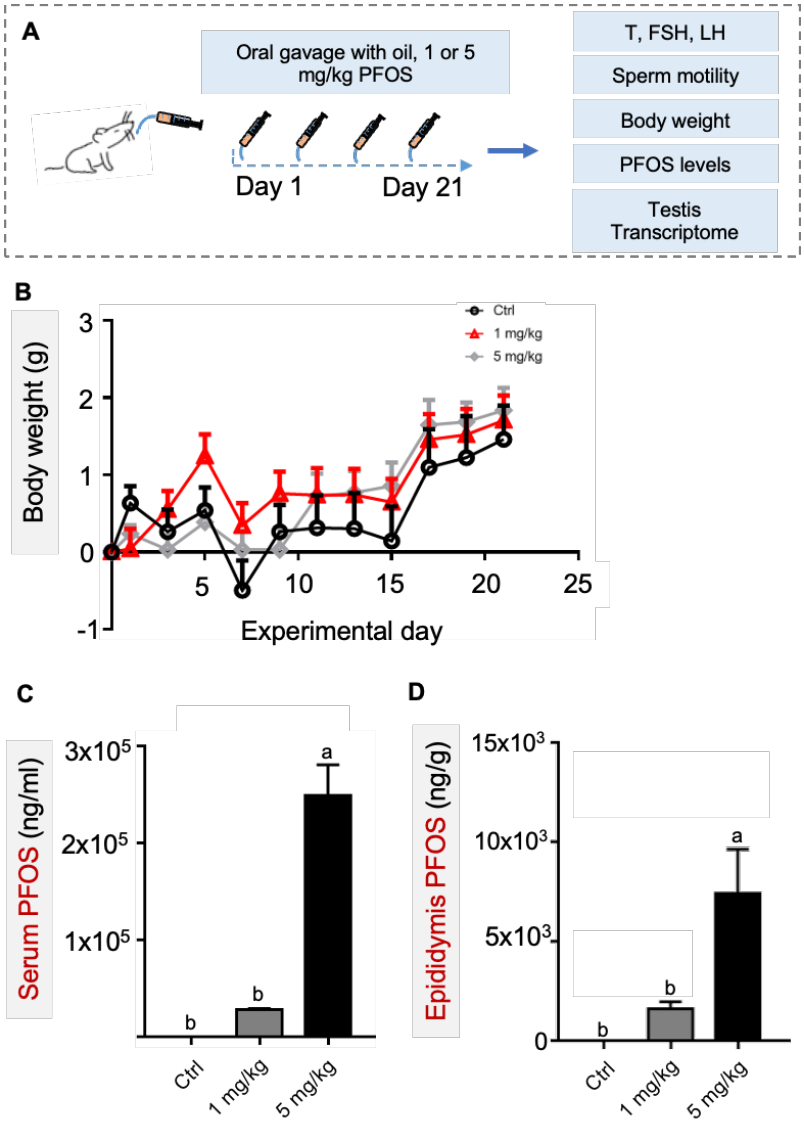

Fig 3.1 PFOS at 1mg/kg and 5mg/kg caused no body weight difference after 21-day treatment.

(A) Animal drug treatment and data analysis workflow. (B) No significant difference in the body weight change was observed in the PFOS treated groups compared with the control group; data were presented as mean ± SEM; n = 10 for the control group; n=15 for the 1 mg/kg PFOS group; n = 15 for the 5 mg/kg PFOS group. (C) PFOS detected in serum at the end of exposure; data were presented as mean mean ± SEM, n = 3 per group; different letters above the bar charts were significantly different according to the results of one-way ANOVA with Tukey's test ($P<0.05$). (D) PFOS detected in epididymis at the end of exposure; data were presented as mean ± SEM, n = 3 per group; different letters above the bar charts were significantly different according to the results of one-way ANOVA with Tukey's test ($P<0.05$).

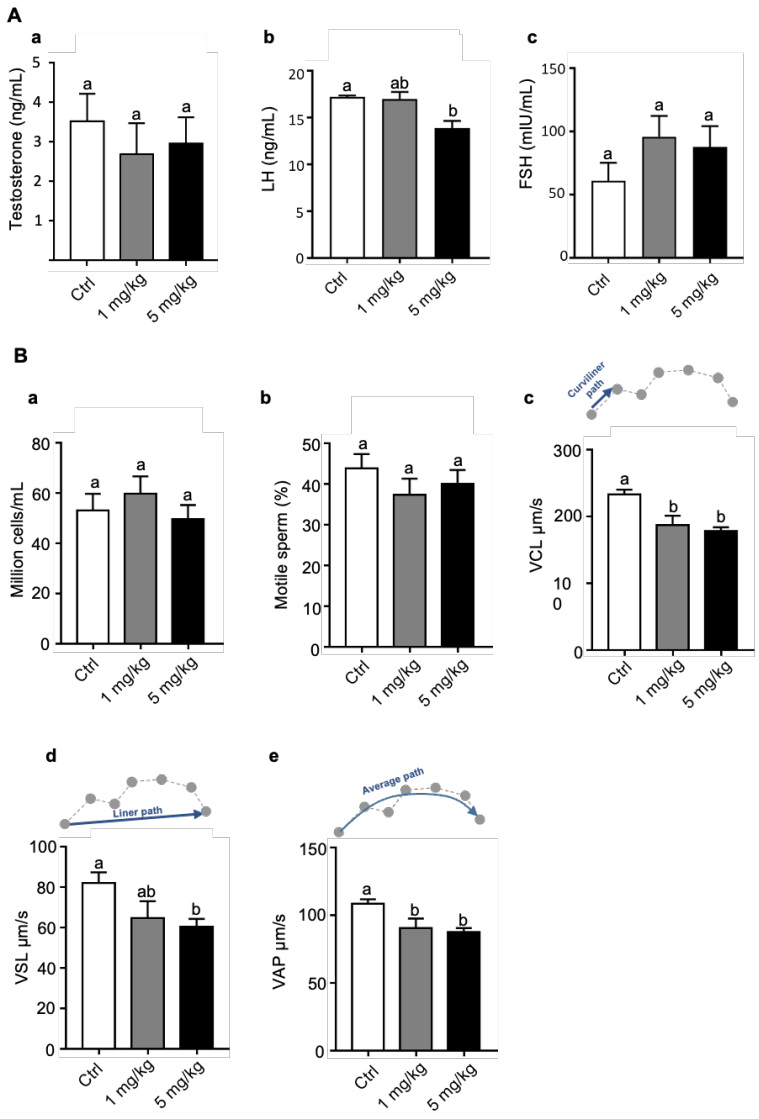

Fig 3.2 PFOS treatment reduced sperm motility and altered LH concentration.

(A) Serum testosterone (T), luteinizing hormone (LH), and follicle-stimulating hormone (FSH) were determined; a. serum testosterone; b. serum luteinizing hormone; c. serum follicle-stimulating hormone; data were presented as mean ± SEM, n = 4 for each group. *P<0.05, ns, not siginficant, One-way ANOVA with Tukey's test. (B) Computer-assisted sperm analysis (CASA) used to analyze epididymal sperm activity; a. total sperm count; b. percentage of motile sperm; c. VCL, curvilinear velocity; d. VSL, straight-line velocity; e. VAP, average path velocity; data were presented as mean ± SEM, n = 7 for the control group, n = 6 for the 1 mg/kg PFOS group, n = 7 for the 5 mg/kg PFOS group; different letters above the bar charts were significantly different according to the results of one-way ANOVA with Tukey's test (p<0.05).

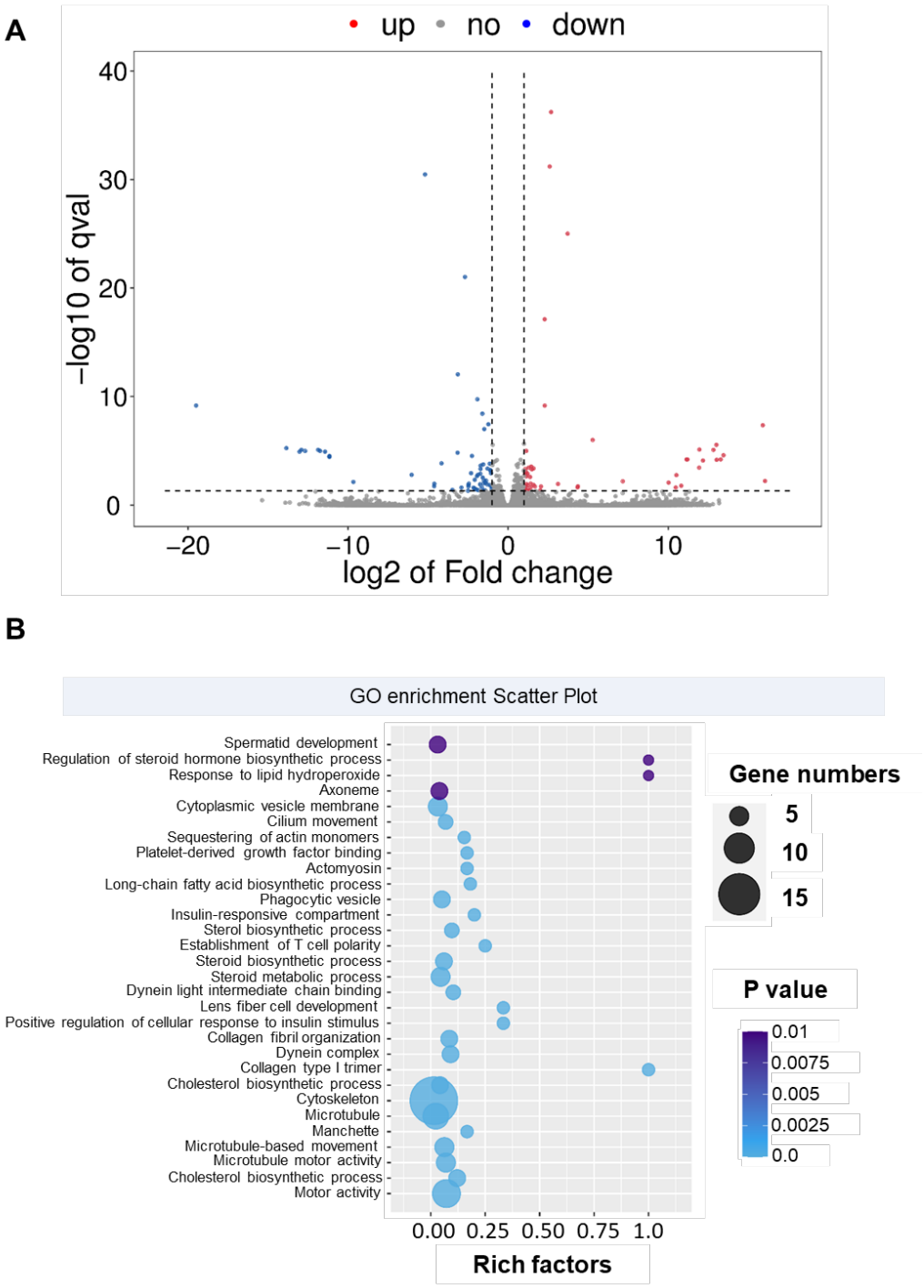

Fig 3.3 PFOS at 5 mg/kg altered the testicular transcriptome after 21-day treatment.

(A) Volcano plot of genes altered by 5 mg/kg PFOS in the testis. Y-axis is -log10 (q-value), x-axis is log2 fold change ratio. Red dots denote significantly up-regulated genes (118), and blue dots denote significantly down-regulated genes (99). (B) Gene Ontology (GO) enrichment plot.

Table 3.2 Gene ontology (GO) enrichment analysis.

Terms	Genes
Motor activity	*Dynlt1f, Dnah10, Kif23, Myo18a, Cenpe, Dync1h1, Myo5a, Dnaic2, Myo1c*
Manchette	*Dync1h1, Rimbp3*
Axoneme	*Spef1, Cfap44, Dnaic2, Dnah10*
Steroid biosynthetic process	*Tm7sf2, Hsd3b1, Mvd, Msmo1*
Long-chain fatty acid biosynthetic process	*Myo5a, Fads1*
Cholesterol metabolic process	*Tm7sf2, Apoa4, Mvd, Msmo1*
Regulation of steroid hormone biosynthetic process	*Lhr*

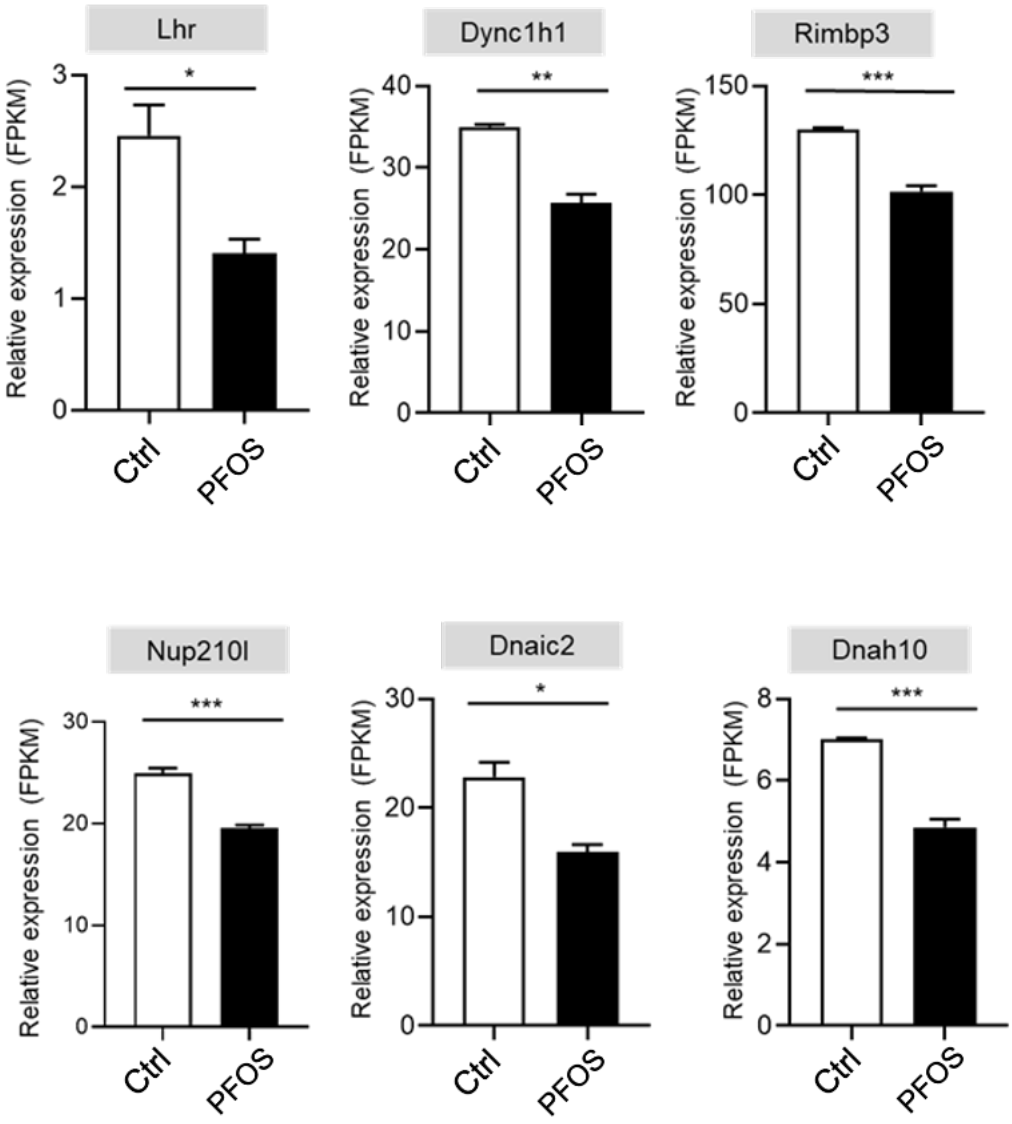

Fig 3.4 RNA-seq Fragments Per Kilobase of transcript per Million mapped reads (FPKM) values in the testes.

FPKM results of *Lhr, Fshr, Dync1h1, Rimbp3, Cfap44, Dnaic2, Dnah10 and Nup210l.* n=3 for each group. *P<0.05, **P<0.01, ***P<0.001, unpaired student's t test.

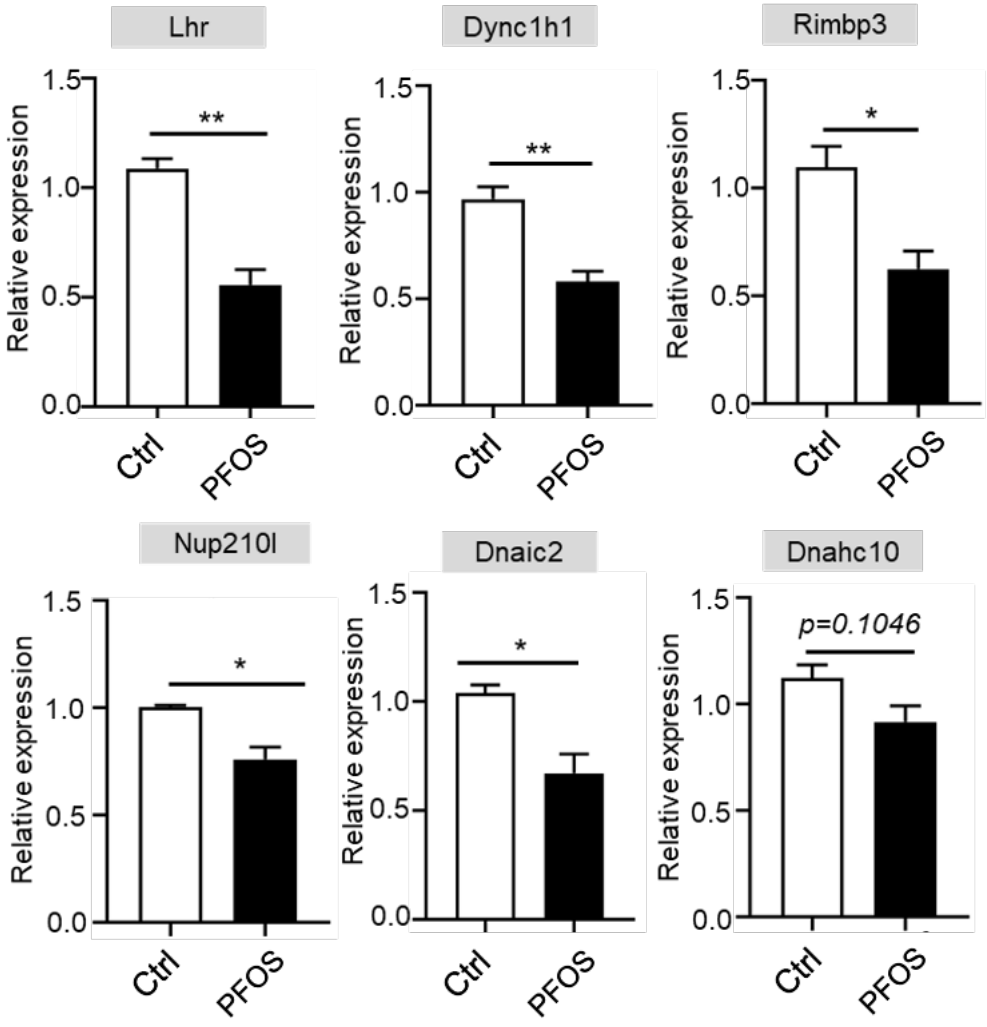

Fig 3.5 Validation of transcriptome results by quantitative real-time PCR (qPCR).

The expression of *Dnaic2, Nup210l, Dync1h1, Rimbp3, Cfap43, Lhr* and *Dnahc10* was measured using qPCR in testes treated with 5 mg/kg PFOS in comparison with the control group. n = 3 for each group.*P<0.05, **P<0.01, unpaired student's t-test.

REFERENCE

1. L. Ritter, K.R.S., J. Forget (November 26, 2010). PERSISTENT ORGANIC POLLUTANTS. An Assessment Report on: DDT Aldrin Dieldrin Endrin Chlordane Heptachlor Hexachlorobenzene Mirex Toxaphene Polychlorinated Biphenyls Dioxins and Furans.
2. Diamanti-Kandarakis, E., Bourguignon, J.P., Giudice, L.C., Hauser, R., Prins, G.S., Soto, A.M., Zoeller, R.T., and Gore, A.C. (2009). Endocrine-disrupting chemicals: an Endocrine Society scientific statement. Endocrine reviews *30*, 293-342. 10.1210/er.2009-0002.
3. Casals-Casas, C., and Desvergne, B. (2011). Endocrine disruptors: from endocrine to metabolic disruption. Annual review of physiology *73*, 135-162. 10.1146/annurev-physiol-012110-142200.
4. Gore, A.C., Chappell, V.A., Fenton, S.E., Flaws, J.A., Nadal, A., Prins, G.S., Toppari, J., and Zoeller, R.T. (2015). EDC-2: The Endocrine Society's Second Scientific Statement on Endocrine-Disrupting Chemicals. Endocrine reviews *36*, E1-e150. 10.1210/er.2015-1010.
5. Banks, R., Smart, B., and Tatlow, J. (1994). Organofluorine chemistry : principles and commercial applications.
6. Buck, R.C., Franklin, J., Berger, U., Conder, J.M., Cousins, I.T., de Voogt, P., Jensen, A.A., Kannan, K., Mabury, S.A., and van Leeuwen, S.P. (2011). Perfluoroalkyl and polyfluoroalkyl substances in the environment: terminology, classification, and origins. Integrated environmental assessment and management *7*, 513-541. 10.1002/ieam.258.
7. Giesy, J.P., and Kannan, K. (2001). Global distribution of perfluorooctane sulfonate in wildlife. Environ Sci Technol *35*, 1339-1342.
8. Liu, J., and Mejia Avendaño, S. (2013). Microbial degradation of polyfluoroalkyl chemicals in the environment: a review. Environ Int *61*, 98-114. 10.1016/j.envint.2013.08.022.

9. Cerro-Gálvez, E., Roscales, J.L., Jiménez, B., Sala, M.M., Dachs, J., and Vila-Costa, M. (2020). Microbial responses to perfluoroalkyl substances and perfluorooctanesulfonate (PFOS) desulfurization in the Antarctic marine environment. Water research *171*, 115434. 10.1016/j.watres.2019.115434.

10. Jiang, X., Wang, J., Deng, X., Xiong, F., Ge, J., Xiang, B., Wu, X., Ma, J., Zhou, M., Li, X., et al. (2019). Role of the tumor microenvironment in PD-L1/PD-1-mediated tumor immune escape. Molecular cancer *18*, 10. 10.1186/s12943-018-0928-4.

11. Yip, S.H., Campos, P., Liu, X., Porteous, R., and Herbison, A.E. (2021). Innervation of GnRH Neuron Distal Projections and Activation by Kisspeptin in a New GnRH-Cre Rat Model. Endocrinology *162*. 10.1210/endocr/bqaa186.

12. Kannan, K., Tao, L., Sinclair, E., Pastva, S.D., Jude, D.J., and Giesy, J.P. (2005). Perfluorinated compounds in aquatic organisms at various trophic levels in a Great Lakes food chain. Archives of environmental contamination and toxicology *48*, 559-566. 10.1007/s00244-004-0133-x.

13. Rovira, J., Martínez, M.Á., Sharma, R.P., Espuis, T., Nadal, M., Kumar, V., Costopoulou, D., Vassiliadou, I., Leondiadis, L., Domingo, J.L., and Schuhmacher, M. (2019). Prenatal exposure to PFOS and PFOA in a pregnant women cohort of Catalonia, Spain. Environ Res *175*, 384-392. 10.1016/j.envres.2019.05.040.

14. Zeng, X.W., Qian, Z., Vaughn, M., Xian, H., Elder, K., Rodemich, E., Bao, J., Jin, Y.H., and Dong, G.H. (2015). Human serum levels of perfluorooctane sulfonate (PFOS) and perfluorooctanoate (PFOA) in Uyghurs from Sinkiang-Uighur Autonomous Region, China: background levels study. Environmental science and pollution research international *22*, 4736-4746. 10.1007/s11356-014-3728-4.

15. Liu, J., Li, J., Zhao, Y., Wang, Y., Zhang, L., and Wu, Y. (2010). The occurrence of perfluorinated alkyl compounds in human milk from different regions of China. Environment international *36*, 433-438. 10.1016/j.envint.2010.03.004.

16. (EFSA), E.F.S.A. (2015). Scientific Opinion on the safety of caffeine. EFSA Journal *13*. 10.2903/j.efsa.2015.4102.

17. Luo, Z., Shi, X., Hu, Q., Zhao, B., and Huang, M. (2012). Structural Evidence of

Perfluorooctane Sulfonate Transport by Human Serum Albumin. Chemical research in toxicology *25*, 990-992. 10.1021/tx300112p.

18. Chain, E.P.o.C.i.t.F., Knutsen, H.K., Alexander, J., Barregard, L., Bignami, M., Bruschweiler, B., Ceccatelli, S., Cottrill, B., Dinovi, M., Edler, L., et al. (2018). Risk to human health related to the presence of perfluorooctane sulfonic acid and perfluorooctanoic acid in food. EFSA J *16*, e05194. 10.2903/j.efsa.2018.5194.
19. Zhou, Z., Shi, Y., Vestergren, R., Wang, T., Liang, Y., and Cai, Y. (2014). Highly Elevated Serum Concentrations of Perfluoroalkyl Substances in Fishery Employees from Tangxun Lake, China. Environ Sci Technol *48*, 3864-3874. 10.1021/es4057467.
20. Harada, K., Inoue, K., Morikawa, A., Yoshinaga, T., Saito, N., and Koizumi, A. (2005). Renal clearance of perfluorooctane sulfonate and perfluorooctanoate in humans and their species-specific excretion. Environ Res *99*, 253-261. 10.1016/j.envres.2004.12.003.
21. Kataria, A., Trachtman, H., Malaga-Dieguez, L., and Trasande, L. (2015). Association between perfluoroalkyl acids and kidney function in a cross-sectional study of adolescents. Environmental health : a global access science source *14*, 89. 10.1186/s12940-015-0077-9.
22. Harada, K.H., Hashida, S., Kaneko, T., Takenaka, K., Minata, M., Inoue, K., Saito, N., and Koizumi, A. (2007). Biliary excretion and cerebrospinal fluid partition of perfluorooctanoate and perfluorooctane sulfonate in humans. Environmental toxicology and pharmacology *24*, 134-139. 10.1016/j.etap.2007.04.003.
23. Chain, E.Panel o.C.i.t.F., Schrenk, D., Bignami, M., Bodin, L., Chipman, J.K., del Mazo, J., Grasl-Kraupp, B., Hogstrand, C., Hoogenboom, L., Leblanc, J.-C., et al. (2020). Risk to human health related to the presence of perfluoroalkyl substances in food. EFSA Journal *18*, e06223. https://doi.org/10.2903/j.efsa.2020.6223.
24. European Food Safety, A. (2008). Perfluorooctane sulfonate (PFOS), perfluorooctanoic acid (PFOA) and their salts Scientific Opinion of the Panel on Contaminants in the Food chain. EFSA Journal *6*, 653.

https://doi.org/10.2903/j.efsa.2008.653.

25. Seacat, A.M., Thomford, P.J., Hansen, K.J., Olsen, G.W., Case, M.T., and Butenhoff, J.L. (2002). Subchronic toxicity studies on perfluorooctanesulfonate potassium salt in cynomolgus monkeys. Toxicol Sci *68*, 249-264. 10.1093/toxsci/68.1.249.

26. Curran, I., Hierlihy, S.L., Liston, V., Pantazopoulos, P., Nunnikhoven, A., Tittlemier, S., Barker, M., Trick, K., and Bondy, G. (2008). Altered fatty acid homeostasis and related toxicologic sequelae in rats exposed to dietary potassium perfluorooctanesulfonate (PFOS). Journal of toxicology and environmental health. Part A *71*, 1526-1541. 10.1080/15287390802361763.

27. Shipley, J.M., Hurst, C.H., Tanaka, S.S., DeRoos, F.L., Butenhoff, J.L., Seacat, A.M., and Waxman, D.J. (2004). trans-Activation of PPARα and Induction of PPARα Target Genes by Perfluorooctane-Based Chemicals. Toxicological Sciences *80*, 151-160. 10.1093/toxsci/kfh130.

28. Wan, H.T., Zhao, Y.G., Wei, X., Hui, K.Y., Giesy, J.P., and Wong, C.K.C. (2012). PFOS-induced hepatic steatosis, the mechanistic actions on β-oxidation and lipid transport. Biochim Biophys Acta *1820*, 1092-1101. 10.1016/j.bbagen.2012.03.010.

29. Xing, J., Wang, G., Zhao, J., Wang, E., Yin, B., Fang, D., Zhao, J., Zhang, H., Chen, Y.Q., and Chen, W. (2016). Toxicity assessment of perfluorooctane sulfonate using acute and subchronic male C57BL/6J mouse models. Environ Pollut *210*, 388-396. 10.1016/j.envpol.2015.12.008.

30. Khansari, M.R., Yousefsani, B.S., Kobarfard, F., Faizi, M., and Pourahmad, J. (2017). In vitro toxicity of perfluorooctane sulfonate on rat liver hepatocytes: probability of distructive binding to CYP 2E1 and involvement of cellular proteolysis. Environmental Science and Pollution Research *24*, 23382-23388. 10.1007/s11356-017-9908-2.

31. Gallo, V., Leonardi, G., Genser, B., Lopez-Espinosa, M.J., Frisbee, S.J., Karlsson, L., Ducatman, A.M., and Fletcher, T. (2012). Serum perfluorooctanoate (PFOA) and perfluorooctane sulfonate (PFOS) concentrations and liver function

biomarkers in a population with elevated PFOA exposure. Environ Health Perspect *120*, 655-660. 10.1289/ehp.1104436.

32. Zegers-Hochschild, F., Adamson, G.D., Dyer, S., Racowsky, C., de Mouzon, J., Sokol, R., Rienzi, L., Sunde, A., Schmidt, L., Cooke, I.D., et al. (2017). The International Glossary on Infertility and Fertility Care, 2017. Fertility and sterility *108*, 393-406. 10.1016/j.fertnstert.2017.06.005.

33. Agarwal, A., Baskaran, S., Parekh, N., Cho, C.-L., Henkel, R., Vij, S., Arafa, M., Panner Selvam, M.K., and Shah, R. (2021). Male infertility. The Lancet *397*, 319-333. 10.1016/s0140-6736(20)32667-2.

34. Lotti, F., and Maggi, M. (2015). Ultrasound of the male genital tract in relation to male reproductive health. Hum Reprod Update *21*, 56-83. 10.1093/humupd/dmu042.

35. Jouannet, P., Wang, C., Eustache, F., Kold-Jensen, T., and Auger, J. (2001). Semen quality and male reproductive health: the controversy about human sperm concentration decline. APMIS *109*, 333-344.

36. Levine, H., Jørgensen, N., Martino-Andrade, A., Mendiola, J., Weksler-Derri, D., Mindlis, I., Pinotti, R., and Swan, S.H. (2017). Temporal trends in sperm count: a systematic review and meta-regression analysis. Human reproduction update *23*, 646-659. 10.1093/humupd/dmx022.

37. Choy, J.T., and Eisenberg, M.L. (2018). Male infertility as a window to health. Fertil Steril *110*, 810-814. 10.1016/j.fertnstert.2018.08.015.

38. Ortona, E., Pierdominici, M., Maselli, A., Veroni, C., Aloisi, F., and Shoenfeld, Y. (2016). Sex-based differences in autoimmune diseases. Ann Ist Super Sanita *52*, 205-212. 10.4415/ANN_16_02_12.

39. Rouchou, B. (2013). Consequences of infertility in developing countries. Perspect Public Health *133*, 174-179. 10.1177/1757913912472415.

40. Chambers, G.M., Sullivan, E.A., Ishihara, O., Chapman, M.G., and Adamson, G.D. (2009). The economic impact of assisted reproductive technology: a review of selected developed countries. Fertil Steril *91*, 2281-2294.

10.1016/j.fertnstert.2009.04.029.

41. de Kretser, D.M., Loveland, K.L., Meinhardt, A., Simorangkir, D., and Wreford, N. (1998). Spermatogenesis. Hum Reprod *13 Suppl 1*, 1-8. 10.1093/humrep/13.suppl_1.1.

42. Griswold, M.D. (1998). The central role of Sertoli cells in spermatogenesis. Seminars in cell & developmental biology *9*, 411-416. 10.1006/scdb.1998.0203.

43. Mruk, D.D., and Cheng, C.Y. (2015). The Mammalian Blood-Testis Barrier: Its Biology and Regulation. Endocrine reviews *36*, 564-591. 10.1210/er.2014-1101.

44. Zirkin, B.R., and Papadopoulos, V. (2018). Leydig cells: formation, function, and regulation. Biol Reprod *99*, 101-111. 10.1093/biolre/ioy059.

45. Cornwall, G.A. (2009). New insights into epididymal biology and function. Hum Reprod Update *15*, 213-227. 10.1093/humupd/dmn055.

46. Lee, V.H., Lee, L.T., and Chow, B.K. (2008). Gonadotropin-releasing hormone: regulation of the GnRH gene. The FEBS journal *275*, 5458-5478. 10.1111/j.1742-4658.2008.06676.x.

47. Belchetz, P.E., Plant, T.M., Nakai, Y., Keogh, E.J., and Knobil, E. (1978). Hypophysial responses to continuous and intermittent delivery of hypopthalamic gonadotropin-releasing hormone. Science *202*, 631-633. 10.1126/science.100883.

48. de Roux, N., Genin, E., Carel, J.C., Matsuda, F., Chaussain, J.L., and Milgrom, E. (2003). Hypogonadotropic hypogonadism due to loss of function of the KiSS1-derived peptide receptor GPR54. Proc Natl Acad Sci U S A *100*, 10972-10976. 10.1073/pnas.1834399100.

49. Seminara, S.B., Messager, S., Chatzidaki, E.E., Thresher, R.R., Acierno, J.S., Jr., Shagoury, J.K., Bo-Abbas, Y., Kuohung, W., Schwinof, K.M., Hendrick, A.G., et al. (2003). The GPR54 gene as a regulator of puberty. The New England journal of medicine *349*, 1614-1627. 10.1056/NEJMoa035322.

50. Lapatto, R., Pallais, J.C., Zhang, D., Chan, Y.M., Mahan, A., Cerrato, F., Le, W.W., Hoffman, G.E., and Seminara, S.B. (2007). Kiss1-/- mice exhibit more variable hypogonadism than Gpr54-/- mice. Endocrinology *148*, 4927-4936.

10.1210/en.2007-0078.

51. Fraietta, R., Zylberstejn, D.S., and Esteves, S.C. (2013). Hypogonadotropic hypogonadism revisited. Clinics (Sao Paulo, Brazil) *68 Suppl 1*, 81-88. 10.6061/clinics/2013(sup01)09.

52. Topaloglu, A.K., Tello, J.A., Kotan, L.D., Ozbek, M.N., Yilmaz, M.B., Erdogan, S., Gurbuz, F., Temiz, F., Millar, R.P., and Yuksel, B. (2012). Inactivating KISS1 mutation and hypogonadotropic hypogonadism. The New England journal of medicine *366*, 629-635. 10.1056/NEJMoa1111184.

53. Lehman, M.N., Merkley, C.M., Coolen, L.M., and Goodman, R.L. (2010). Anatomy of the kisspeptin neural network in mammals. Brain research *1364*, 90-102. 10.1016/j.brainres.2010.09.020.

54. Akil, H., Watson, S.J., Young, E., Lewis, M.E., Khachaturian, H., and Walker, J.M. (1984). Endogenous opioids: biology and function. Annual review of neuroscience *7*, 223-255. 10.1146/annurev.ne.07.030184.001255.

55. Goodman, R.L., Coolen, L.M., Anderson, G.M., Hardy, S.L., Valent, M., Connors, J.M., Fitzgerald, M.E., and Lehman, M.N. (2004). Evidence that dynorphin plays a major role in mediating progesterone negative feedback on gonadotropin-releasing hormone neurons in sheep. Endocrinology *145*, 2959-2967. 10.1210/en.2003-1305.

56. Navarro, V.M., Gottsch, M.L., Chavkin, C., Okamura, H., Clifton, D.K., and Steiner, R.A. (2009). Regulation of gonadotropin-releasing hormone secretion by kisspeptin/dynorphin/neurokinin B neurons in the arcuate nucleus of the mouse. J Neurosci *29*, 11859-11866. 10.1523/jneurosci.1569-09.2009.

57. True, C., Kirigiti, M., Ciofi, P., Grove, K.L., and Smith, M.S. (2011). Characterisation of arcuate nucleus kisspeptin/neurokinin B neuronal projections and regulation during lactation in the rat. J Neuroendocrinol *23*, 52-64. 10.1111/j.1365-2826.2010.02076.x.

58. Uenoyama, Y., Nagae, M., Tsuchida, H., Inoue, N., and Tsukamura, H. (2021). Role of KNDy Neurons Expressing Kisspeptin, Neurokinin B, and Dynorphin A as a

GnRH Pulse Generator Controlling Mammalian Reproduction. Front Endocrinol (Lausanne) *12*, 724632. 10.3389/fendo.2021.724632.

59. Son, Y.L., Ubuka, T., Millar, R.P., Kanasaki, H., and Tsutsui, K. (2012). Gonadotropin-inhibitory hormone inhibits GnRH-induced gonadotropin subunit gene transcriptions by inhibiting AC/cAMP/PKA-dependent ERK pathway in LβT2 cells. Endocrinology *153*, 2332-2343. 10.1210/en.2011-1904.

60. Tsutsui, K., and Ubuka, T. (2018). How to Contribute to the Progress of Neuroendocrinology: Discovery of GnIH and Progress of GnIH Research. Front Endocrinol (Lausanne) *9*, 662. 10.3389/fendo.2018.00662.

61. Tsutsui, K., Saigoh, E., Ukena, K., Teranishi, H., Fujisawa, Y., Kikuchi, M., Ishii, S., and Sharp, P.J. (2000). A novel avian hypothalamic peptide inhibiting gonadotropin release. Biochem Biophys Res Commun *275*, 661-667. 10.1006/bbrc.2000.3350.

62. Rizwan, M.Z., Porteous, R., Herbison, A.E., and Anderson, G.M. (2009). Cells Expressing RFamide-Related Peptide-1/3, the Mammalian Gonadotropin-Inhibitory Hormone Orthologs, Are Not Hypophysiotropic Neuroendocrine Neurons in the Rat. Endocrinology *150*, 1413-1420. 10.1210/en.2008-1287 %J Endocrinology.

63. Ubuka, T., Inoue, K., Fukuda, Y., Mizuno, T., Ukena, K., Kriegsfeld, L.J., and Tsutsui, K. (2012). Identification, Expression, and Physiological Functions of Siberian Hamster Gonadotropin-Inhibitory Hormone. Endocrinology *153*, 373-385. 10.1210/en.2011-1110 %J Endocrinology.

64. Spencer, R.L., and Deak, T. (2017). A users guide to HPA axis research. Physiology & behavior *178*, 43-65. 10.1016/j.physbeh.2016.11.014.

65. Nargund, V.H. (2015). Effects of psychological stress on male fertility. Nat Rev Urol *12*, 373-382. 10.1038/nrurol.2015.112.

66. Chandran, U.R., Attardi, B., Friedman, R., Dong, K.W., Roberts, J.L., and DeFranco, D.B. (1994). Glucocorticoid receptor-mediated repression of gonadotropin-releasing hormone promoter activity in GT1 hypothalamic cell lines. Endocrinology *134*, 1467-1474. 10.1210/endo.134.3.8119188.

67. Wang, O. (2012). Glucocorticoids Regulate Kisspeptin Neurons during Stress and Contribute to Infertility and Obesity in Leptin-Deficient Mice. Doctoral dissertation, Harvard University.

68. Kotitschke, A., Sadie-Van Gijsen, H., Avenant, C., Fernandes, S., and Hapgood, J.P. (2009). Genomic and nongenomic cross talk between the gonadotropin-releasing hormone receptor and glucocorticoid receptor signaling pathways. Molecular endocrinology (Baltimore, Md.) *23*, 1726-1745. 10.1210/me.2008-0462.

69. Suter, D.E., and Schwartz, N.B. (1985). Effects of glucocorticoids on secretion of luteinizing hormone and follicle-stimulating hormone by female rat pituitary cells in vitro. Endocrinology *117*, 849-854. 10.1210/endo-117-3-849.

70. Hu, G.X., Lian, Q.Q., Lin, H., Latif, S.A., Morris, D.J., Hardy, M.P., and Ge, R.S. (2008). Rapid mechanisms of glucocorticoid signaling in the Leydig cell. Steroids *73*, 1018-1024. 10.1016/j.steroids.2007.12.020.

71. Andric, S.A., Kojic, Z., Bjelic, M.M., Mihajlovic, A.I., Baburski, A.Z., Sokanovic, S.J., Janjic, M.M., Stojkov, N.J., Stojilkovic, S.S., and Kostic, T.S. (2013). The opposite roles of glucocorticoid and α1-adrenergic receptors in stress triggered apoptosis of rat Leydig cells. American journal of physiology. Endocrinology and metabolism *304*, E51-59. 10.1152/ajpendo.00443.2012.

72. Lopez-Espinosa, M.J., Mondal, D., Armstrong, B.G., Eskenazi, B., and Fletcher, T. (2016). Perfluoroalkyl Substances, Sex Hormones, and Insulin-like Growth Factor-1 at 6-9 Years of Age: A Cross-Sectional Analysis within the C8 Health Project. Environ Health Perspect *124*, 1269-1275. 10.1289/ehp.1509869.

73. Lopez-Espinosa, M.J., Fletcher, T., Armstrong, B., Genser, B., Dhatariya, K., Mondal, D., Ducatman, A., and Leonardi, G. (2011). Association of Perfluorooctanoic Acid (PFOA) and Perfluorooctane Sulfonate (PFOS) with age of puberty among children living near a chemical plant. Environ Sci Technol *45*, 8160-8166. 10.1021/es1038694.

74. Du, G., Hu, J., Huang, Z., Yu, M., Lu, C., Wang, X., and Wu, D. (2019). Neonatal and juvenile exposure to perfluorooctanoate (PFOA) and perfluorooctane sulfonate

(PFOS): Advance puberty onset and kisspeptin system disturbance in female rats. Ecotoxicol Environ Saf *167*, 412-421. 10.1016/j.ecoenv.2018.10.025.

75. Zhao, B., Li, L., Liu, J., Li, H., Zhang, C., Han, P., Zhang, Y., Yuan, X., Ge, R.S., and Chu, Y. (2014). Exposure to perfluorooctane sulfonate in utero reduces testosterone production in rat fetal Leydig cells. PloS one *9*, e78888. 10.1371/journal.pone.0078888.

76. Wan, H.T., Zhao, Y.G., Wong, M.H., Lee, K.F., Yeung, W.S.B., Giesy, J.P., and Wong, C.K.C. (2011). Testicular signaling is the potential target of perfluorooctanesulfonate-mediated subfertility in male mice. Biol Reprod *84*, 1016-1023. 10.1095/biolreprod.110.089219.

77. Qu, J.H., Lu, C.C., Xu, C., Chen, G., Qiu, L.L., Jiang, J.K., Ben, S., Wang, Y.B., Gu, A.H., and Wang, X.R. (2016). Perfluorooctane sulfonate-induced testicular toxicity and differential testicular expression of estrogen receptor in male mice. Environmental toxicology and pharmacology *45*, 150-157. 10.1016/j.etap.2016.05.025.

78. Kaur, G., Mital, P., and Dufour, J.M. (2013). Testisimmune privilege - Assumptions versus facts. Animal reproduction *10*, 3-15.

79. Qiu, L., Qian, Y., Liu, Z., Wang, C., Qu, J., Wang, X., and Wang, S. (2016). Perfluorooctane sulfonate (PFOS) disrupts blood-testis barrier by down-regulating junction proteins via p38 MAPK/ATF2/MMP9 signaling pathway. Toxicology *373*. 10.1016/j.tox.2016.11.003.

80. Li, N., Mruk, D.D., Chen, H., Wong, C.K., Lee, W.M., and Cheng, C.Y. (2016). Rescue of perfluorooctanesulfonate (PFOS)-mediated Sertoli cell injury by overexpression of gap junction protein connexin 43. Sci Rep *6*, 29667. 10.1038/srep29667.

81. Wan, H.T., Mruk, D.D., Wong, C.K., and Cheng, C.Y. (2014). Perfluorooctanesulfonate (PFOS) perturbs male rat Sertoli cell blood-testis barrier function by affecting F-actin organization via p-FAK-Tyr(407): an in vitro study. Endocrinology *155*, 249-262. 10.1210/en.2013-1657.

82. Lai, K.P., Lee, J.C., Wan, H.T., Li, J.W., Wong, A.Y., Chan, T.F., Oger, C., Galano, J.M., Durand, T., Leung, K.S., et al. (2017). Effects of in Utero PFOS Exposure on Transcriptome, Lipidome, and Function of Mouse Testis. Environ Sci Technol *51*, 8782-8794. 10.1021/acs.est.7b02102.

83. Alam, M.N., Han, X., Nan, B., Liu, L., Tian, M., Shen, H., and Huang, Q. (2021). Chronic low-level perfluorooctane sulfonate (PFOS) exposure promotes testicular steroidogenesis through enhanced histone acetylation. Environ Pollut *284*, 117518. 10.1016/j.envpol.2021.117518.

84. Feng, X., Wang, X., Cao, X., Xia, Y., Zhou, R., and Chen, L. (2015). Chronic Exposure of Female Mice to an Environmental Level of Perfluorooctane Sulfonate Suppresses Estrogen Synthesis Through Reduced Histone H3K14 Acetylation of the StAR Promoter Leading to Deficits in Follicular Development and Ovulation. Toxicol Sci *148*, 368-379. 10.1093/toxsci/kfv197.

85. Maestri, L., Negri, S., Ferrari, M., Ghittori, S., Fabris, F., Danesino, P., and Imbriani, M. (2006). Determination of perfluorooctanoic acid and perfluorooctanesulfonate in human tissues by liquid chromatography/single quadrupole mass spectrometry. Rapid communications in mass spectrometry : RCM *20*, 2728-2734. 10.1002/rcm.2661.

86. Ahrens, L., Siebert, U., and Ebinghaus, R. (2009). Total body burden and tissue distribution of polyfluorinated compounds in harbor seals (Phoca vitulina) from the German Bight. Marine pollution bulletin *58*, 520-525. 10.1016/j.marpolbul.2008.11.030.

87. Olivero-Verbel, J., Tao, L., Johnson-Restrepo, B., Guette-Fernández, J., Baldiris-Avila, R., O'Byrne-Hoyos, I., and Kannan, K. (2006). Perfluorooctanesulfonate and related fluorochemicals in biological samples from the north coast of Colombia. Environ Pollut *142*, 367-372. 10.1016/j.envpol.2005.09.022.

88. Yu, Y., Wang, C., Zhang, X., Zhu, J., Wang, L., Ji, M., Zhang, Z., Ji, X.M., and Wang, S.L. (2020). Perfluorooctane sulfonate disrupts the blood brain barrier through the crosstalk between endothelial cells and astrocytes in mice. Environ Pollut *256*,

113429. 10.1016/j.envpol.2019.113429.

89. Austin, M.E., Kasturi, B.S., Barber, M., Kannan, K., MohanKumar, P.S., and MohanKumar, S.M.J. (2003). Neuroendocrine effects of perfluorooctane sulfonate in rats. Environmental health perspectives *111*, 1485-1489.

90. Cui, L., Zhou, Q.F., Liao, C.Y., Fu, J.J., and Jiang, G.B. (2009). Studies on the toxicological effects of PFOA and PFOS on rats using histological observation and chemical analysis. Archives of environmental contamination and toxicology *56*, 338-349. 10.1007/s00244-008-9194-6.

91. Wang, X., Li, B., Zhao, W.-D., Liu, Y.-J., Shang, D.-S., Fang, W.-G., and Chen, Y.-H. (2011). Perfluorooctane sulfonate triggers tight junction "opening" in brain endothelial cells via phosphatidylinositol 3-kinase. Biochem Biophys Res Commun *410*, 258-263. 10.1016/j.bbrc.2011.05.128.

92. Rhea, E.M., and Banks, W.A. (2019). Role of the Blood-Brain Barrier in Central Nervous System Insulin Resistance. *13*. 10.3389/fnins.2019.00521.

93. Chen, N., Li, J., Li, D., Yang, Y., and He, D. (2014). Chronic exposure to perfluorooctane sulfonate induces behavior defects and neurotoxicity through oxidative damages, in vivo and in vitro. PloS one *9*, e113453. 10.1371/journal.pone.0113453.

94. Chen, X., Nie, X., Mao, J., Zhang, Y., Yin, K., and Jiang, S. (2018). Perfluorooctanesulfonate induces neuroinflammation through the secretion of TNF-α mediated by the JAK2/STAT3 pathway. NeuroToxicology *66*, 32-42. https://doi.org/10.1016/j.neuro.2018.03.003.

95. Kim, Y.-K., Na, K.-S., Myint, A.-M., and Leonard, B.E. (2016). The role of pro-inflammatory cytokines in neuroinflammation, neurogenesis and the neuroendocrine system in major depression. Progress in Neuro-Psychopharmacology and Biological Psychiatry *64*, 277-284. https://doi.org/10.1016/j.pnpbp.2015.06.008.

96. Johansson, N., Eriksson, P., and Viberg, H. (2009). Neonatal exposure to PFOS and PFOA in mice results in changes in proteins which are important for neuronal

growth and synaptogenesis in the developing brain. Toxicol Sci *108*, 412-418. 10.1093/toxsci/kfp029.

97. Ye, S., Kim, J.-i., Kim, J., and Kaang, B.-K. (2019). Overexpression of activated CaMKII in the CA1 hippocampus impairs context discrimination, but not contextual conditioning. Molecular Brain *12*, 32. 10.1186/s13041-019-0454-3.

98. Benowitz, L.I., and Routtenberg, A. (1997). GAP-43: an intrinsic determinant of neuronal development and plasticity. Trends in Neurosciences *20*, 84-91. https://doi.org/10.1016/S0166-2236(96)10072-2.

99. Adams, D.J., Arthur, C.P., and Stowell, M.H.B. (2015). Architecture of the Synaptophysin/Synaptobrevin Complex: Structural Evidence for an Entropic Clustering Function at the Synapse. Scientific Reports *5*, 13659. 10.1038/srep13659.

100. Kwon, S.E., and Chapman, E.R. (2011). Synaptophysin regulates the kinetics of synaptic vesicle endocytosis in central neurons. Neuron *70*, 847-854. 10.1016/j.neuron.2011.04.001.

101. Rubenstein, J.L., Greengard, P., and Czernik, A.J. (1993). Calcium-dependent serine phosphorylation of synaptophysin. Synapse (New York, N.Y.) *13*, 161-172. 10.1002/syn.890130207.

102. Liu, X., Liu, W., Jin, Y., Yu, W., Liu, L., and Yu, H. (2010). Effects of subchronic perfluorooctane sulfonate exposure of rats on calcium-dependent signaling molecules in the brain tissue. Archives of toxicology *84*, 471-479. 10.1007/s00204-010-0517-9.

103. Long, Y., Wang, Y., Ji, G., Yan, L., Hu, F., and Gu, A. (2013). Neurotoxicity of perfluorooctane sulfonate to hippocampal cells in adult mice. PLoS One *8*, e54176. 10.1371/journal.pone.0054176.

104. Wang, Y., and Jin, Y. (2012). Perfluorooctane sulfonate (PFOS) and calcium channel downstream signaling molecules. Toxicology Research *1*, 103-107. 10.1039/c2tx20017a.

105. Foguth, R.M., Flynn, R.W., de Perre, C., Iacchetta, M., Lee, L.S., Sepúlveda, M.S.,

and Cannon, J.R. (2019). Developmental exposure to perfluorooctane sulfonate (PFOS) and perfluorooctanoic acid (PFOA) selectively decreases brain dopamine levels in Northern leopard frogs. Toxicology and Applied Pharmacology *377*, 114623. https://doi.org/10.1016/j.taap.2019.114623.

106. Wang, X., Bai, Y., Tang, C., Cao, X., Chang, F., and Chen, L. (2018). Impact of Perfluorooctane Sulfonate on Reproductive Ability of Female Mice through Suppression of Estrogen Receptor α-Activated Kisspeptin Neurons. Toxicol Sci *165*, 475-486. 10.1093/toxsci/kfy167.

107. Sato, I., Kawamoto, K., Nishikawa, Y., Tsuda, S., Yoshida, M., Yaegashi, K., Saito, N., Liu, W., and Jin, Y. (2009). Neurotoxicity of perfluorooctane sulfonate (PFOS) in rats and mice after single oral exposure. J Toxicol Sci *34*, 569-574. 10.2131/jts.34.569.

108. Wang, Y., Liu, W., Zhang, Q., Zhao, H., and Quan, X. (2015). Effects of developmental perfluorooctane sulfonate exposure on spatial learning and memory ability of rats and mechanism associated with synaptic plasticity. Food Chem Toxicol *76*, 70-76. 10.1016/j.fct.2014.12.008.

109. Flament-Durand, J. (1980). The hypothalamus: anatomy and functions. Acta psychiatrica Belgica *80*, 364-375.

110. López-Doval, S., Salgado, R., Pereiro, N., Moyano, R., and Lafuente, A. (2014). Perfluorooctane sulfonate effects on the reproductive axis in adult male rats. Environ Res *134*, 158-168. 10.1016/j.envres.2014.07.006.

111. Bao, M., Zheng, S., Liu, C., Huang, W., Xiao, J., and Wu, K. (2020). Perfluorooctane sulfonate exposure alters sexual behaviors and transcriptions of genes in hypothalamic–pituitary–gonadal–liver axis of male zebrafish (Danio rerio). Environmental Pollution *267*, 115585. https://doi.org/10.1016/j.envpol.2020.115585.

112. López-Doval, S., Salgado, R., and Lafuente, A. (2016). The expression of several reproductive hormone receptors can be modified by perfluorooctane sulfonate (PFOS) in adult male rats. Chemosphere *155*, 488-497.

https://doi.org/10.1016/j.chemosphere.2016.04.081.

113. Yu, N., Wei, S., Li, M., Yang, J., Li, K., Jin, L., Xie, Y., Giesy, J.P., Zhang, X., and Yu, H. (2016). Effects of Perfluorooctanoic Acid on Metabolic Profiles in Brain and Liver of Mouse Revealed by a High-throughput Targeted Metabolomics Approach. Sci Rep *6*, 23963. 10.1038/srep23963.

114. Johansson, N., Fredriksson, A., and Eriksson, P. (2008). Neonatal exposure to perfluorooctane sulfonate (PFOS) and perfluorooctanoic acid (PFOA) causes neurobehavioural defects in adult mice. Neurotoxicology *29*, 160-169. 10.1016/j.neuro.2007.10.008.

115. Spulber, S., Kilian, P., Wan Ibrahim, W.N., Onishchenko, N., Ulhaq, M., Norrgren, L., Negri, S., Di Tuccio, M., and Ceccatelli, S. (2014). PFOS induces behavioral alterations, including spontaneous hyperactivity that is corrected by dexamfetamine in zebrafish larvae. PloS one *9*, e94227. 10.1371/journal.pone.0094227.

116. Hoffman, K., Webster, T.F., Weisskopf, M.G., Weinberg, J., and Vieira, V.M. (2010). Exposure to polyfluoroalkyl chemicals and attention deficit/hyperactivity disorder in U.S. children 12-15 years of age. Environmental health perspectives *118*, 1762-1767. 10.1289/ehp.1001898.

117. Fuentes, S., Vicens, P., Colomina, M.T., and Domingo, J.L. (2007). Behavioral effects in adult mice exposed to perfluorooctane sulfonate (PFOS). Toxicology *242*, 123-129. https://doi.org/10.1016/j.tox.2007.09.012.

118. Pang, Z., Chong, J., Zhou, G., de Lima Morais, D.A., Chang, L., Barrette, M., Gauthier, C., Jacques, P., Li, S., and Xia, J. (2021). MetaboAnalyst 5.0: narrowing the gap between raw spectra and functional insights. Nucleic acids research *49*, W388-w396. 10.1093/nar/gkab382.

119. López-Ibáñez, J., Pazos, F., and Chagoyen, M. (2016). MBROLE 2.0-functional enrichment of chemical compounds. Nucleic acids research *44*, W201-204. 10.1093/nar/gkw253.

120. Ouagazzal, A.M., Kenny, P.J., and File, S.E. (1999). Stimulation of nicotinic

receptors in the lateral septal nucleus increases anxiety. The European journal of neuroscience *11*, 3957-3962. 10.1046/j.1460-9568.1999.00823.x.

121. Liang, H.Y., Chen, Z.J., Xiao, H., Lin, Y.H., Hu, Y.Y., Chang, L., Wu, H.Y., Wang, P., Lu, W., Zhu, D.Y., and Luo, C.X. (2020). nNOS-expressing neurons in the vmPFC transform pPVT-derived chronic pain signals into anxiety behaviors. Nature communications *11*, 2501. 10.1038/s41467-020-16198-5.

122. McCall, J.G., Al-Hasani, R., Siuda, E.R., Hong, D.Y., Norris, A.J., Ford, C.P., and Bruchas, M.R. (2015). CRH Engagement of the Locus Coeruleus Noradrenergic System Mediates Stress-Induced Anxiety. Neuron *87*, 605-620. 10.1016/j.neuron.2015.07.002.

123. Li, L., Feng, X., Zhou, Z., Zhang, H., Shi, Q., Lei, Z., Shen, P., Yang, Q., Zhao, B., Chen, S., et al. (2018). Stress Accelerates Defensive Responses to Looming in Mice and Involves a Locus Coeruleus-Superior Colliculus Projection. Curr Biol *28*, 859-871.e855. 10.1016/j.cub.2018.02.005.

124. Onishchenko, N., Fischer, C., Wan Ibrahim, W.N., Negri, S., Spulber, S., Cottica, D., and Ceccatelli, S. (2011). Prenatal Exposure to PFOS or PFOA Alters Motor Function in Mice in a Sex-Related Manner. Neurotoxicity Research *19*, 452-461. 10.1007/s12640-010-9200-4.

125. Ojo, A.F., Peng, C., and Ng, J.C. (2021). Assessing the human health risks of per- and polyfluoroalkyl substances: A need for greater focus on their interactions as mixtures. Journal of Hazardous Materials *407*, 124863. https://doi.org/10.1016/j.jhazmat.2020.124863.

126. Yuan, Z., Shao, X., Miao, Z., Zhao, B., Zheng, Z., and Zhang, J. (2018). Perfluorooctane sulfonate induced neurotoxicity responses associated with neural genes expression, neurotransmitter levels and acetylcholinesterase activity in planarians Dugesia japonica. Chemosphere *206*, 150-156. 10.1016/j.chemosphere.2018.05.011.

127. Li, W., He, Q.Z., Wu, C.Q., Pan, X.Y., Wang, J., Tan, Y., Shan, X.Y., and Zeng, H.C. (2015). PFOS Disturbs BDNF-ERK-CREB Signalling in Association with Increased

MicroRNA-22 in SH-SY5Y Cells. BioMed research international *2015*, 302653. 10.1155/2015/302653.

128. Dong, X., Yang, J., Nie, X., Xiao, J., and Jiang, S. (2016). Perfluorooctane sulfonate (PFOS) impairs the proliferation of C17.2 neural stem cells via the downregulation of GSK-3β/β-catenin signaling. Journal of applied toxicology : JAT *36*, 1591-1598. 10.1002/jat.3320.

129. Ge, J., Wang, C., Nie, X., Yang, J., Lu, H., Song, X., Su, K., Li, T., Han, J., Zhang, Y., et al. (2016). ROS-mediated apoptosis of HAPI microglia through p53 signaling following PFOS exposure. Environmental toxicology and pharmacology *46*, 9-16. 10.1016/j.etap.2016.06.025.

130. Sun, P., Nie, X., Chen, X., Yin, L., Luo, J., Sun, L., Wan, C., and Jiang, S. (2018). Nrf2 Signaling Elicits a Neuroprotective Role Against PFOS-mediated Oxidative Damage and Apoptosis. Neurochemical research *43*, 2446-2459. 10.1007/s11064-018-2672-y.

131. Yu, N., Wei, S., Li, M., Yang, J., Li, K., Jin, L., Xie, Y., Giesy, J.P., Zhang, X., and Yu, H. (2016). Effects of Perfluorooctanoic Acid on Metabolic Profiles in Brain and Liver of Mouse Revealed by a High-throughput Targeted Metabolomics Approach. Sci Rep *6*, 23963. 10.1038/srep23963.

132. Ognjenović, J., and Simonović, M. (2018). Human aminoacyl-tRNA synthetases in diseases of the nervous system. RNA biology *15*, 623-634. 10.1080/15476286.2017.1330245.

133. Fleming, E.W., Tewari, S., and Noble, E.P. (1975). Effects of chronic ethanol ingestion on brain aminoacyl-tRNA synthestases and tRNA. Journal of neurochemistry *24*, 553-560. 10.1111/j.1471-4159.1975.tb07674.x.

134. Hasegawa, K., Omata, S., and Sugano, H. (1988). In vivo and in vitro effects of methylmercury on the activities of aminoacyl-tRNA synthetases in rat brain. Archives of toxicology *62*, 470-472. 10.1007/bf00288352.

135. Zhao, P., Hou, K., Yang, S., and Xia, X. (2020). Characterization of small metabolites alteration in mice brain tissues after infected by rabies virus. Infection,

genetics and evolution : journal of molecular epidemiology and evolutionary genetics in infectious diseases *85*, 104571. 10.1016/j.meegid.2020.104571.

136. Löscher, W., and Potschka, H. (2005). Blood-brain barrier active efflux transporters: ATP-binding cassette gene family. NeuroRx : the journal of the American Society for Experimental NeuroTherapeutics *2*, 86-98. 10.1602/neurorx.2.1.86.

137. Begley, D.J. (2004). ABC transporters and the blood-brain barrier. Curr Pharm Des *10*, 1295-1312.

138. Vogelgesang, S., Cascorbi, I., Schroeder, E., Pahnke, J., Kroemer, H.K., Siegmund, W., Kunert-Keil, C., Walker, L.C., and Warzok, R.W. (2002). Deposition of Alzheimer's beta-amyloid is inversely correlated with P-glycoprotein expression in the brains of elderly non-demented humans. Pharmacogenetics *12*, 535-541. 10.1097/00008571-200210000-00005.

139. Bartels, A.L., Willemsen, A.T., Kortekaas, R., de Jong, B.M., de Vries, R., de Klerk, O., van Oostrom, J.C., Portman, A., and Leenders, K.L. (2008). Decreased blood-brain barrier P-glycoprotein function in the progression of Parkinson's disease, PSP and MSA. Journal of neural transmission (Vienna, Austria : 1996) *115*, 1001-1009. 10.1007/s00702-008-0030-y.

140. Aronica, E., Sisodiya, S.M., and Gorter, J.A. (2012). Cerebral expression of drug transporters in epilepsy. Advanced drug delivery reviews *64*, 919-929. 10.1016/j.addr.2011.11.008.

141. Maes, M., Verkerk, R., Vandoolaeghe, E., Lin, A., and Scharpé, S. (1998). Serum levels of excitatory amino acids, serine, glycine, histidine, threonine, taurine, alanine and arginine in treatment-resistant depression: modulation by treatment with antidepressants and prediction of clinical responsivity. Acta psychiatrica Scandinavica *97*, 302-308. 10.1111/j.1600-0447.1998.tb10004.x.

142. Yu, M.C., Wang, T.M., Chiou, Y.H., Yu, M.K., Lin, C.F., and Chiu, C.Y. (2021). Urine metabolic phenotyping in children with nocturnal enuresis and comorbid neurobehavioral disorders. Sci Rep *11*, 16592. 10.1038/s41598-021-96104-1.

143. Paul, A.G., Jones, K.C., and Sweetman, A.J. (2009). A first global production,

emission, and environmental inventory for perfluorooctane sulfonate. Environ Sci Technol *43*, 386-392.

144. Liu, Z., Lu, Y., Wang, P., Wang, T., Liu, S., Johnson, A.C., Sweetman, A.J., and Baninla, Y. (2017). Pollution pathways and release estimation of perfluorooctane sulfonate (PFOS) and perfluorooctanoic acid (PFOA) in central and eastern China. Sci Total Environ *580*, 1247-1256. 10.1016/j.scitotenv.2016.12.085.

145. Zeng, Z., Song, B., Xiao, R., Zeng, G., Gong, J., Chen, M., Xu, P., Zhang, P., Shen, M., and Yi, H. (2019). Assessing the human health risks of perfluorooctane sulfonate by in vivo and in vitro studies. Environment International *126*, 598-610. 10.1016/j.envint.2019.03.002.

146. Qiu, L., Wang, H., Dong, T., Huang, J., Li, T., Ren, H., Wang, X., Qu, J., and Wang, S. (2021). Perfluorooctane sulfonate (PFOS) disrupts testosterone biosynthesis via CREB/CRTC2/StAR signaling pathway in Leydig cells. Toxicology *449*, 152663. 10.1016/j.tox.2020.152663.

147. Toft, G., Jönsson, B.A., Lindh, C.H., Giwercman, A., Spano, M., Heederik, D., Lenters, V., Vermeulen, R., Rylander, L., Pedersen, H.S., et al. (2012). Exposure to perfluorinated compounds and human semen quality in Arctic and European populations. Hum Reprod *27*, 2532-2540. 10.1093/humrep/des185.

148. Song, X., Tang, S., Zhu, H., Chen, Z., Zang, Z., Zhang, Y., Niu, X., Wang, X., Yin, H., Zeng, F., and He, C. (2018). Biomonitoring PFAAs in blood and semen samples: Investigation of a potential link between PFAAs exposure and semen mobility in China. Environ Int *113*, 50-54. 10.1016/j.envint.2018.01.010.

149. Raymer, J.H., Michael, L.C., Studabaker, W.B., Olsen, G.W., Sloan, C.S., Wilcosky, T., and Walmer, D.K. (2012). Concentrations of perfluorooctane sulfonate (PFOS) and perfluorooctanoate (PFOA) and their associations with human semen quality measurements. Reprod Toxicol *33*, 419-427. 10.1016/j.reprotox.2011.05.024.

150. Khezri, A., Lindeman, B., Krogenæs, A.K., Berntsen, H.F., Zimmer, K.E., and Ropstad, E. (2017). Maternal exposure to a mixture of persistent organic pollutants (POPs) affects testis histology, epididymal sperm count and induces sperm DNA

fragmentation in mice. Toxicology and Applied Pharmacology *329*, 301-308. https://doi.org/10.1016/j.taap.2017.06.019.

151. Lessard, M., Herst, P.M., Charest, P.L., Navarro, P., Joly-Beauparlant, C., Droit, A., Kimmins, S., Trasler, J., Benoit-Biancamano, M.-O., MacFarlane, A.J., et al. (2019). Prenatal Exposure to Environmentally-Relevant Contaminants Perturbs Male Reproductive Parameters Across Multiple Generations that are Partially Protected by Folic Acid Supplementation. Scientific Reports *9*, 13829. 10.1038/s41598-019-50060-z.

152. Mao, B., Mruk, D., Lian, Q., Ge, R., Li, C., Silvestrini, B., and Cheng, C.Y. (2018). Mechanistic Insights into PFOS-Mediated Sertoli Cell Injury. Trends Mol Med *24*, 781-793. 10.1016/j.molmed.2018.07.001.

153. Gao, Y., Chen, H., Xiao, X., Lui, W.-y., Lee, W.M., Mruk, D.D., and Cheng, C.Y. (2017). Perfluorooctanesulfonate (PFOS)-induced Sertoli cell injury through a disruption of F-actin and microtubule organization is mediated by Akt1/2. Scientific Reports *7*, 1110. 10.1038/s41598-017-01016-8.

154. Wan, H.T., Lai, K.P., and Wong, C.K.C. (2020). Comparative Analysis of PFOS and PFOA Toxicity on Sertoli Cells. Environ Sci Technol *54*, 3465-3475. 10.1021/acs.est.0c00201.

155. Ashizawa, K., Wishart, G.J., Nishinakama, K., Sakamoto, T., and Tsuzuki, Y. (1995). Regulatory mechanisms of fowl sperm motility: possible role of endogenous myosin light chain kinase-like protein. Journal of reproduction and fertility *104*, 141-148. 10.1530/jrf.0.1040141.

156. Lehti, M.S., Zhang, F.P., Kotaja, N., and Sironen, A. (2017). SPEF2 functions in microtubule-mediated transport in elongating spermatids to ensure proper male germ cell differentiation. Development (Cambridge, England) *144*, 2683-2693. 10.1242/dev.152108.

157. Wen, Q., Tang, E.I., Lui, W.Y., Lee, W.M., Wong, C.K.C., Silvestrini, B., and Cheng, C.Y. (2018). Dynein 1 supports spermatid transport and spermiation during spermatogenesis in the rat testis. American journal of physiology. Endocrinology

and metabolism *315*, E924-e948. 10.1152/ajpendo.00114.2018.

158. Huang, J., Sun, L., Mennigen, J.A., Liu, Y., Liu, S., Zhang, M., Wang, Q., and Tu, W. (2021). Developmental toxicity of the novel PFOS alternative OBS in developing zebrafish: An emphasis on cilia disruption. Journal of Hazardous Materials *409*, 124491. https://doi.org/10.1016/j.jhazmat.2020.124491.

159. Zhou, J., Du, Y.R., Qin, W.H., Hu, Y.G., Huang, Y.N., Bao, L., Han, D., Mansouri, A., and Xu, G.L. (2009). RIM-BP3 is a manchette-associated protein essential for spermiogenesis. Development (Cambridge, England) *136*, 373-382. 10.1242/dev.030858.

160. Arafah, K., Lopez, F., Cazin, C., Kherraf, Z.-E., Tassistro, V., Loundou, A., Arnoult, C., Thierry-Mieg, N., Bulet, P., Guichaoua, M.-R., and Ray, P.F. (2020). Defect in the nuclear pore membrane glycoprotein 210-like gene is associated with extreme uncondensed sperm nuclear chromatin and male infertility: a case report. Human Reproduction *36*, 693-701. 10.1093/humrep/deaa329 %J Human Reproduction.

161. Stanifer, J.W., Stapleton, H.M., Souma, T., Wittmer, A., Zhao, X., and Boulware, L.E. (2018). Perfluorinated Chemicals as Emerging Environmental Threats to Kidney Health: A Scoping Review. Clin J Am Soc Nephrol *13*, 1479-1492. 10.2215/CJN.04670418.

162. Qazi, M.R., Abedi, M.R., Nelson, B.D., DePierre, J.W., and Abedi-Valugerdi, M. (2010). Dietary exposure to perfluorooctanoate or perfluorooctane sulfonate induces hypertrophy in centrilobular hepatocytes and alters the hepatic immune status in mice. International immunopharmacology *10*, 1420-1427. 10.1016/j.intimp.2010.08.009.

163. Kishi, R., Nakajima, T., Goudarzi, H., Kobayashi, S., Sasaki, S., Okada, E., Miyashita, C., Itoh, S., Araki, A., Ikeno, T., et al. (2015). The Association of Prenatal Exposure to Perfluorinated Chemicals with Maternal Essential and Long-Chain Polyunsaturated Fatty Acids during Pregnancy and the Birth Weight of Their Offspring: The Hokkaido Study. Environ Health Perspect *123*, 1038-1045. 10.1289/ehp.1408834.

164. Sèdes, L., Thirouard, L., Maqdasy, S., Garcia, M., Caira, F., Lobaccaro, J.A., Beaudoin, C., and Volle, D.H. (2018). Cholesterol: A Gatekeeper of Male Fertility? Front Endocrinol (Lausanne) *9*, 369. 10.3389/fendo.2018.00369.

165. Collodel, G., Castellini, C., Lee, J.C.-Y., and Signorini, C. (2020). Relevance of Fatty Acids to Sperm Maturation and Quality. Oxid Med Cell Longev *2020*, 7038124-7038124. 10.1155/2020/7038124.

166. Fleming, A.D., and Yanagimachi, R. (1984). Evidence suggesting the importance of fatty acids and the fatty acid moieties of sperm membrane phospholipids in the acrosome reaction of guinea pig spermatozoa. The Journal of experimental zoology *229*, 485-489. 10.1002/jez.1402290317.

167. Meizel, S., and Turner, K.O. (1983). Stimulation of an exocytotic event, the hamster sperm acrosome reaction, by cis-unsaturated fatty acids. FEBS Lett *161*, 315-318. 10.1016/0014-5793(83)81032-1.

168. Hosseini, B., Nourmohamadi, M., Hajipour, S., Taghizadeh, M., Asemi, Z., Keshavarz, S.A., and Jafarnejad, S. (2019). The Effect of Omega-3 Fatty Acids, EPA, and/or DHA on Male Infertility: A Systematic Review and Meta-analysis. Journal of dietary supplements *16*, 245-256. 10.1080/19390211.2018.1431753.

169. Tavilani, H., Doosti, M., Abdi, K., Vaisiraygani, A., and Joshaghani, H.R. (2006). Decreased polyunsaturated and increased saturated fatty acid concentration in spermatozoa from asthenozoospermic males as compared with normozoospermic males. Andrologia *38*, 173-178. 10.1111/j.1439-0272.2006.00735.x.

170. Martínez-Soto, J.C., Landeras, J., and Gadea, J. (2013). Spermatozoa and seminal plasma fatty acids as predictors of cryopreservation success. Andrology *1*, 365-375. 10.1111/j.2047-2927.2012.00040.x.

CURRICULUM VITAE

Academic qualifications of the thesis author, Mr. LI Zijie:

— Received the degree of Bachelor of Science from South China Agriculture University, June 2019.

March 2022